

Arene Activation with Mercury(II) and Thallium(III) Electrophiles. Mechanistic Relevance of Charge-Transfer Transitions in π -Complexes as Intermediates

W. Lau and J. K. Kochi*

Contribution from the Department of Chemistry, University of Houston, University Park, Houston, Texas 77004. Received April 14, 1986

Abstract: The activation of various aromatic hydrocarbons by mercuration and thallation proceeds via π -complexes, as observed by the transient charge-transfer (CT) absorption spectra. Quantitative spectrophotometric analysis of (a) the association constants K and (b) the second-order rate constants k_2 establishes the reactive forms of the electrophiles to be $\text{Hg}(\text{O}_2\text{CCF}_3)_2$ and $\text{Tl}(\text{O}_2\text{CCF}_3)_2^+$, both in π -complex formation as well as in aromatic metalation. The direct participation by these isoelectronic and isostructural species presents a unique opportunity to examine arene activation with electrophiles which primarily differ only in the charge they bear. A detailed comparison of the CT excitation energies and the reactivities of various arenes relative to steric, kinetic isotope, and solvent effects in mercuration and thallation reveals unusual similarities. At the same time the observation of arene cations as key intermediates in thallation, but not in mercuration, leads to puzzling incongruities. The paradox is analyzed in the context of merging stepwise (electron-transfer) and concerted (electrophilic) mechanisms.

The homogeneous activation of aromatic carbon-hydrogen bonds is readily effected by electrophilic metal complexes, especially those of mercury(II), thallium(III), and lead(IV).¹⁻⁹ Despite the extensive synthetic uses of mercuration and thallation,¹⁰ there are only limited mechanistic studies of the metalations of arenes.^{11,12} In particular there is little known quantitatively about the extent to which the activation barriers for mercuration and thallation are related and how they are differentiated.^{13,14}

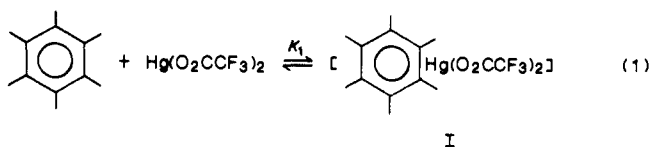
We recently demonstrated the presence of arene-thallium(III) π -complexes as reaction intermediates and described how the associated charge-transfer absorption bands can be used to delineate competing electrophilic and electron-transfer pathways in aromatic thallation.^{15,16} In this study we examine the analogous

π -complexes of mercury(II) as a basis for the quantitative comparison of thallation with mercuration under identical reaction conditions. We utilize the Benesi-Hildebrand analysis for complex formation with the complete kinetics in order to expand on earlier studies of Olah, Roberts, and co-workers for the treatment of a series of arenes with mercury(II) and thallium(III) trifluoroacetates.^{13,14}

Results

I. Formation of Transient π -Complexes of Arenes with Mercury(II) Trifluoroacetate. A fleeting yellow color is observed when a solution of mesitylene is mixed with an equimolar amount of mercury(II) trifluoroacetate. The absorption spectrum shown in Figure 1 consists of a broad band in the region ($\lambda > 300$ nm) in which neither component alone absorbs. The position of the absorption band changes systematically with the ionization potential (IP) of the methylbenzene—the trend varying in the order hexamethylbenzene < pentamethylbenzene < 1,2,4,5-tetramethylbenzene < mesitylene. Such a spectral shift to progressively higher energies with the increase in the ionization potential of the methylbenzene, as listed in Table I, accords with the charge-transfer origin of these new absorption bands.^{18,19}

The controlled removal of the solvent from an equimolar mixture of hexamethylbenzene and mercury(II) trifluoroacetate dissolved in either methylene chloride or trifluoroacetic acid afforded a quantitative yield of pale-yellow single crystals of the 1:1 complex I.²⁰ X-ray crystallography established the dihapto



bonding of mercury to the aromatic ring via two unusually long Hg-C distances of 2.56 and 2.58 Å expected for weak π -interactions in such electron donor-acceptor complexes.^{21,22} Most importantly, the comparison of the absorption spectrum of the crystalline complex I with that measured in dichloromethane

(1) Makarova, L. G.; Nesmeyanov, A. N. In *Methods of Elemento-organic Chemistry*; Nesmeyanov, A. N., Kocheskov, K. A., Eds.; North-Holland, Amsterdam, 1967; Vol. 4.

(2) (a) Kitching, W. *Organomet. Chem. Rev.* **1968**, *3*, 35. (b) Taylor, R. In *Comprehensive Chemical Kinetics*; Bamford, C. H., Tipper, C. F. H., Eds.; Elsevier: Amsterdam, **1972**; Vol. 13, p 186 ff.

(3) Wardell, J. L. *Comp. Organomet. Chem.* **1982**, *2*, 874.

(4) (a) McKillop, A.; Taylor, E. C. *Adv. Organomet. Chem.* **1973**, *11*, 147; *Acc. Chem. Res.* **1970**, *3*, 338; *Chem. Ber.* **1973**, *9*, 4. (b) McKillop, A. *Pure Appl. Chem.* **1975**, *43*, 463. (c) McKillop, A.; Hunt, J. D.; Zelesko, M. J.; Fowler, J. S.; Taylor, E. C.; McGillivray, G.; Kienzle, F. *J. Am. Chem. Soc.* **1971**, *93*, 4841.

(5) (a) Ouellette, R. J. In *Oxidation in Organic Chemistry: Part B*; Trahanovsky, W. S., Ed.; Academic: New York, **1973**; p. 135 ff. (b) Nesmeyanov, A. N.; Kocheskov, K. A., ref 1, Vol. 4.

(6) McKillop, A.; Taylor, E. C. *Comp. Organomet. Chem.* **1982**, *7*, 499.

(7) Criegee, R., In *Oxidation in Organic Chemistry*; Wiberg, K. B., Ed.; Academic: New York, 1965; Vol 5-A, p 326 ff.

(8) Campbell, J. R.; Kallman, J. R.; Pinhey, J. T.; Sternhell, S. *Tetrahedron Lett.* **1972**, 1763; **1973**, 5369.

(9) For other metals, see: Aoyama, Y.; Yoshida, T.; Sakurai, K.; Ogoshi H. *Organometallics* **1986**, *5*, 168.

(10) See studies by: (a) Larock, R. C.; Harrison, L. W. *J. Am. Chem. Soc.* **1984**, *106*, 4218 and related papers. (b) Taylor, E. C.; Conley, R. A.; Katz, A. H.; McKillop, A. *J. Org. Chem.* **1984**, *49*, 3840 and related papers.

(11) (a) Perrin, C.; Westheimer, F. H. *J. Am. Chem. Soc.* **1963**, *85*, 2773 and related papers. (b) Kresge, A. J.; Dubeck, M.; Brown, H. C.; Wirkkala, R. A. *J. Am. Chem. Soc.* **1966**, *88*, 1447, 1453, 1456. Brown, H. C. *J. Org. Chem.* **1967**, *32*, 745 and related papers. (c) For a recent review, see ref 3.

(12) (a) Taylor, E. C.; Kienzle, F.; Robey, R. L.; McKillop, A.; Hunt, J. D. *J. Am. Chem. Soc.* **1971**, *93*, 4845 and related papers. (b) Kwok, P. Y.; Stock, L. M.; Wright, T. L. *J. Org. Chem.* **1979**, *44*, 2309. (c) For a recent review, see ref 6.

(13) Fung, C. W.; Khorramdel-Vahed, M.; Ranson, R. J.; Roberts, R. M. *J. Chem. Soc., Perkin Trans. 2* **1980**, 267.

(14) Olah, G. A.; Hashimoto, I.; Lin, H. C. *Proc. Natl. Acad. Sci. U.S.A.* **1977**, *74*, 4121.

(15) Lau, W.; Kochi, J. K. *J. Am. Chem. Soc.* **1984**, *106*, 7100.

(16) In this study, we use the terms π -complex and EDA complex interchangeably. For the confusion regarding the definition of π -complex, see footnote 5 in ref 17.

(17) Fukuzumi, S.; Kochi, J. K. *J. Am. Chem. Soc.* **1981**, *103*, 7240.

(18) Mulliken, R. S.; Person, W. B. *Molecular Complexes*, Wiley-Interscience: New York, 1969.

(19) Foster, R. *Organic Charge-Transfer Complexes*; Academic: New York, 1969.

(20) Lau, W.; Huffman, J. C.; Kochi, J. K. *J. Am. Chem. Soc.* **1982**, *104*, 5515.

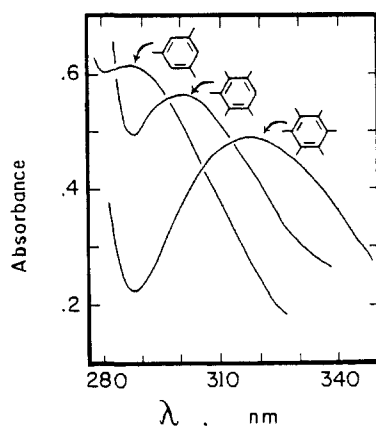
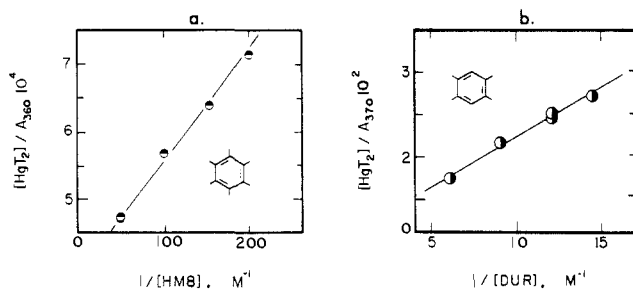
(21) Prout, C. K.; Kamenar, B. *Mol. Complexes* **1973**, *1*, 151.

(22) Soos, Z. G.; Klein, D. J. *Mol. Assoc.* **1972**, *1*, 2.

Table I. Charge-Transfer Absorptions of the π -Complexes of Various Methylarenes with Mercury(II) Trifluoroacetate

methylbenzene	ionization potential, eV	dichloromethane			trifluoroacetic acid		
		$\lambda,^a$ nm	$\epsilon_{CT}, M^{-1} cm^{-1}$	K_1, M^{-1}	$\lambda,^a$ nm	$\epsilon_{CT}, M^{-1} cm^{-1}$	K_1, M^{-1}
hexamethyl	7.85	323	2320	16	360	2538	250
pentamethyl	7.92	355	495	13			170 ^b
1,2,4,5-tetramethyl	8.05	335	489	8.1	370	585	62
1,2,3,5-tetramethyl	8.07	340	503	9.0			84 ^b
1,2,3,4-tetramethyl	8.14	345	374	9.3			89 ^b
1,2,3-trimethyl	8.42	325	647	4.7	355	1501	22
1,2,4-trimethyl	8.27	320	709	4.2	355	1343	19
1,3,5-trimethyl	8.42	335	395	5.1			28 ^b
1,2-dimethyl	8.56	300	999	3.5	310	3492	17
toluene	8.82	300	383	2.1	310	1865	5.1
benzene	9.23	295	190	0.91	300	947	1.5

^a Monitoring wavelength of the CT band and extinction coefficient ϵ_{CT} . For Benesi-Hildebrand treatment, typical concentrations are 4×10^{-3} – 2×10^{-2} M $Hg(O_2CCF_3)_2$ and 5×10^{-2} – 5×10^{-1} M arene in CH_2Cl_2 and 1 – 2×10^{-3} M $Hg(O_2CCF_3)_2$ and 1 – 5×10^{-2} M arene in trifluoroacetic acid.
^b From Figure 4 by interpolation with data in CH_2Cl_2 .

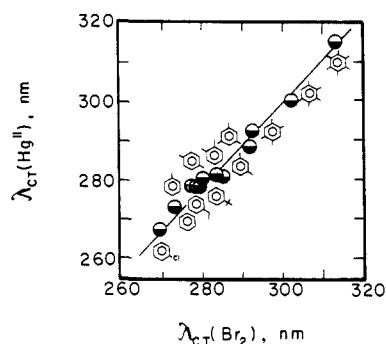
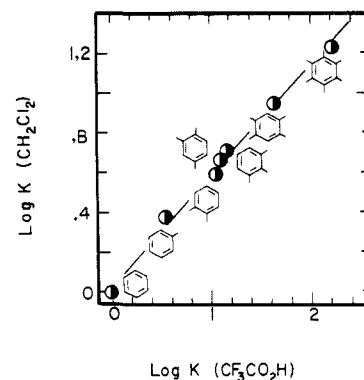

Figure 1. Typical charge-transfer spectra of π -complexes from hexamethylbenzene (2.5×10^{-3} M), pentamethylbenzene (2.5×10^{-3} M), and mesitylene (5.0×10^{-3} M) with equimolar amounts of $Hg(O_2CCF_3)_2$ in dichloromethane at $-40^\circ C$.

Figure 2. Typical Benesi-Hildebrand plots of (a) hexamethylbenzene and (b) durene with mercury(II) trifluoroacetate in trifluoroacetic acid at $\lambda = 340$ and 370 nm.

indicates that the charge-transfer transition is the same in the solid state and in solution.

The association constant K_1 of the π -complex in solution was measured by the spectrophotometric procedure of Benesi and Hildebrand.^{23,24} Thus, for the formation of the 1:1 complex as given in eq 1, the change in the CT absorbance A_{CT} with concentration variations is given by eq 2 where HgT_2 and ArH

$$\frac{[Hg(O_2CCF_3)_2]}{A_{CT}} = \frac{1}{\epsilon_{CT}} + \frac{1}{K_1 \epsilon_{CT}} [ArH]^{-1} \quad (2)$$

represent mercury(II) trifluoroacetate and hexamethylbenzene, respectively, under conditions in which the donor is present in excess. The fit of the absorbance data to this formulation is shown in Figure 2. The slope of the line is given by $[K_1 \epsilon_{CT}]^{-1}$ and the


Figure 3. Correlation of the CT bands of the π -complexes of mercury(II) trifluoroacetate and bromine with various arenes in trifluoroacetic acid.

Figure 4. Solvent effects on equilibria. Correlation of the association constants K_1 for π -complex formation of mercury(II) trifluoroacetate with various arenes in CH_2Cl_2 and CF_3CO_2H .

intercept is $1/\epsilon_{CT}$, both of which were found to be independent of the monitoring wavelength in the region between 350 and 380 nm. The same method was used to evaluate the association constants of the other arenes listed in Table I. Since the CT bands in these cases were transient, precautions were always taken to measure the absorbances immediately after mixing the components and extrapolating the data to zero time. It is noteworthy that the magnitudes of both K_1 and ϵ_{CT} increase with the donor properties of the arene.^{19,25} Although the π -complex of hexamethylbenzene (which has no aromatic hydrogens) is persistent, the results in Figure 1 and Table I demonstrate that it is not otherwise differentiated from the other methylarenes in its charge-transfer properties. Such a conclusion is confirmed by the strong correspondence of these charge-transfer bands with those of the well-known electron donor-acceptor complexes of the same series of arenes with molecular bromine (see Figure 3).²⁶

(23) Benesi, H. A.; Hildebrand, J. H. *J. Am. Chem. Soc.* **1949**, *71*, 2703.

(24) Person, W. B. *J. Am. Chem. Soc.* **1965**, *87*, 167.

(25) Foster, R. F. *Mol. Complexes* **1974**, *2*, 251.

(26) Fukuzumi, S.; Kochi, J. K. *J. Org. Chem.* **1981**, *46*, 4116.

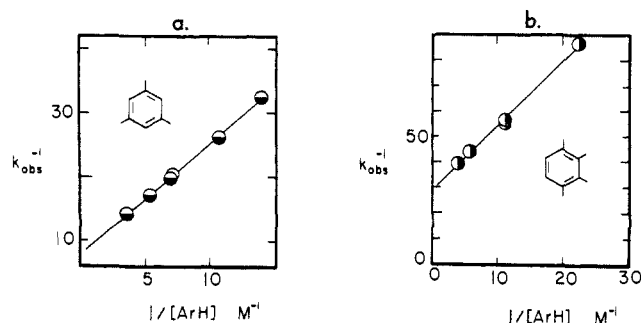


Figure 5. Typical kinetics for the mercuration of (a) mesitylene and (b) 1,2,3,4-tetramethylbenzene in CH_2Cl_2 according to eq 6.

When dichloromethane is replaced by trifluoroacetic acid as the solvent, the maximum of the CT band of the hexamethylbenzene complex undergoes a substantial blue shift from 315 to 305 nm. Such a solvent effect is similar to that previously observed in the π -complexes of arenes with molecular bromine.²⁶ A hypsochromic shift by a constant amount of $\sim 4 \text{ kcal mol}^{-1}$ was observed for a series of arene complexes in the two media. The magnitudes of the association constants are also similarly affected by the solvent, as shown by the linear correlation in Figure 4. However, the slope of less than unity indicates that the perturbation of the π -complex by solvent is not constant but increases monotonically with the donor properties of the methylarene. Furthermore, the CT absorption band of a solution containing an equimolar mixture of $2.5 \times 10^{-3} \text{ M}$ mercury(II) trifluoroacetate and hexamethylbenzene in trifluoroacetic acid remained singularly unchanged by the presence of up to 0.01 M lithium trifluoroacetate. Thus, the ionic dissociation of the electron acceptor, i.e., eq 3, is not involved in the formation of the π -complex (vide infra).



Otherwise, the effect of trifluoroacetic acid on the π -complex, particularly the blue shift in the CT spectra and the increase in the association constant, is best considered in the context of the preferential solvation of the arene moiety.²⁷⁻²⁹

II. Kinetics of Arene Mercuration with Mercury(II) Trifluoroacetate. The disappearance of the CT absorption band coincided with the mercuration of the arene. The mercuration products were isolated in excellent yields according to the stoichiometry¹¹ in eq 4. Hexamethylbenzene was the only methy-



larene which did not react under these thermal conditions. (The photoinduced reaction obtained upon the irradiation of the CT band of the hexamethylbenzene complex is described separately.³¹) The rates of mercuration were measured spectrophotometrically in dichloromethane by following the decay of the CT absorption band at various wavelengths. In the presence of excess arene donor, the mercuration followed first-order kinetics to more than 90% completion. The pseudo-first-order rate constant k_{obsd} was independent of the monitoring wavelength. Coupled with the absence of ionic dissociation of mercury(II) trifluoroacetate (eq 3) during π -complex formation (vide supra), the kinetic studies indicate an attack of the undissociated $\text{Hg}(\text{O}_2\text{CCF}_3)_2$ on the arene during mercuration. The relationship between the experimental

Table II. Kinetics of Mercuration in Dichloromethane^a

methylbenzene	λ , ^b nm	K_1 , M^{-1}	$10^2 k_1$, s^{-1}	k_2 , ^c $\text{M}^{-1} \text{s}^{-1}$	rel rate ^d
1,3,5-trimethyl	335	4.4	12.9	0.57	1.0
1,2,4-trimethyl	320	6.9	1.32	0.091	0.16
1,2,3-trimethyl	325	8.8	1.48	0.13	0.23
1,2,3,4-tetramethyl	345	11.4	3.44	0.39	0.68
1,2,3,5-tetramethyl	340	11.9	9.12	1.1	1.9
1,2,4,5-tetramethyl	335	9.6	0.93	0.089	0.16
pentamethyl	355	13.6	8.51	1.2	2.0

^a In 2 mL of dichloromethane containing 0.004–0.02 M $\text{Hg}(\text{O}_2\text{CCF}_3)_2$ and 0.05–0.5 M methylarene at 25 °C. ^b Wavelength of monitoring light for the disappearance of the CT band. ^c As k_2 .³² ^d Relative to mesitylene.

Table III. Kinetics of Mercuration in Trifluoroacetic Acid^a

methylbenzene	λ , ^b nm	k_2 , ^c $\text{M}^{-1} \text{s}^{-1}$	rel rate ^d
1,3-dimethyl	320	2.3	1.0
1,3,5-trimethyl	345	31	13
1,2,4-trimethyl	355	3.6	1.6
1,2,3-trimethyl	355	4.4	1.9
1,2,4,6-tetramethyl	370	4.3	1.9

^a In 2 mL of trifluoroacetic acid containing $2.0 \times 10^{-3} \text{ M}$ $\text{Hg}(\text{O}_2\text{CCF}_3)_2$ and 0.02–0.08 M methylarene at 25 °C. ^b Wavelength of monitoring light for the disappearing of the CT band. ^c From $k_{\text{obsd}}[\text{ArH}]^{-1}$ averaged at greater than or equal to five arene concentrations. ^d Relative to *m*-xylene.

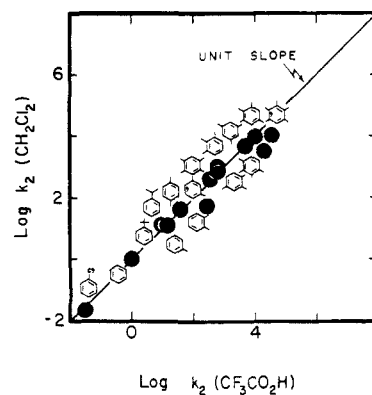
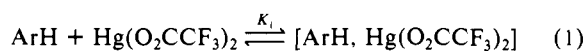


Figure 6. Solvent effects on the kinetics. Correlation of the second-order rate constants for mercuration in dichloromethane and trifluoroacetic acid.

rate constant for such a process and the concentration of the arene is shown in Figure 5 for a pair of typical examples. The dependences of the reciprocal quantities were consistently found to be linear with a correlation coefficient of >0.99 . Such a result is readily accommodated by the formulation in Scheme I. The

Scheme I



experimental rate constant k_{obsd} relates to each step of Scheme I as in eq 6 under conditions in which $[\text{ArH}] \gg [\text{Hg}(\text{O}_2\text{CCF}_3)_2]$.¹³

$$\frac{1}{k_{\text{obsd}}} = \frac{1}{k_1} + \frac{1}{K_1 k_1 [\text{ArH}]} \quad (6)$$

Accordingly, the rate-limiting rate constant k_1 and the preequilibrium association constant K_1 can be obtained from the slopes and intercepts, respectively, of plots such as those shown in Figure 5. The values of the K_1 and k_1 are listed in Table II (columns 3 and 4) for various methylbenzenes together with the overall second-order rate constant k_2 (column 5).³² It is singularly

(32) The overall second-order rate constant taken as $k_2 \sim k_1 K_1$ is especially applicable when the magnitude of K_1 is limited.

(27) Davis, K. M. C. *Mol. Assoc.* **1975**, *1*, 151.

(28) Dannenberg, J. J. *Angew. Chem., Int. Ed. Engl.* **1975**, *14*, 641.

(29) (a) Note that arene solvation by trifluoroacetic acid differs from protonation by strong acids such as trifluoromethanesulfonic acid. The latter affords the σ -adduct or benzenium ion as indicated by the appearance of a pair of new absorption bands, ~ 300 and 400 nm , when $\text{CF}_3\text{SO}_3\text{H}$ is added to a dichloromethane solution of hexamethylbenzene. (b) Compare the absorption of heptamethylbenzenium ion at 287 and 397 nm.³⁰ (c) See also: Mackor, E. L.; Hofstra, A.; van der Waals, J. H. *Trans. Faraday Soc.* **1958**, *54*, 66, 187. And Brown, H. C.; McGary, C. W., Jr. *J. Am. Chem. Soc.* **1955**, *77*, 2300.

(30) (a) Doering, W. von E.; Saunders, M.; Boyton, H. G.; Earhart, H. W.; Wadley, E. F.; Edwards, W. R.; Laber, G. *Tetrahedron* **1958**, *4*, 178. (b) See also: Baenziger, N. C.; Nelson, A. D. *J. Am. Chem. Soc.* **1968**, *90*, 6602.

(31) Lau, W.; Kochi, J. K. *J. Org. Chem.* **1986**, *51*, 1801.

Table IV. Relative Reactivities of Arenes Toward Mercuration in Dichloromethane and Trifluoroacetic Acid^a

substituted benzene	CH ₂ Cl ₂ ^b	CF ₃ CO ₂ H ^c	substituted benzene	CH ₂ Cl ₂ ^b	CF ₃ CO ₂ H ^c
pentamethyl	9400	3 7900	1,4-dimethyl	39	41
1,2,4,5-tetramethyl	720	670	1,2-dimethyl	48	340
1,2,3,5-tetramethyl	8800	11 600	<i>tert</i> -butyl	13	10
1,2,3,4-tetramethyl	3200	19 800	isopropyl	12	14
1,2,3-trimethyl	1100	690	ethyl	10	15
1,2,4-trimethyl	740	580	methyl	10	18
1,3,5-trimethyl	4600	4 900	none	1	1.0
1,3-dimethyl	430	360	chloro	0.02	0.03

^aSecond-order rate constants evaluated relative to that of benzene at 25 °C. ^bChlorobenzene to mesitylene from ref 17. Mesitylene to pentamethylbenzene from Table II. Relative rates of the two are related via mesitylene. ^cFrom ref 14 and Table III. Prehnitene, isodurene, and pentamethylbenzene are related via mesitylene.

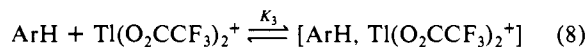
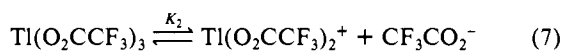
noteworthy that the values of the association constant K_1 evaluated by this kinetics procedure are essentially the same as those obtained under static conditions from the Benesi-Hildebrand treatment of the spectrophotometric data (see Table I).

The rates of mercuration in trifluoroacetic acid were consistently faster than those measured in dichloromethane. Coupled with the significantly large magnitudes of the association constant in this medium (see Table I), the procedure described in eq 6 was difficult to manipulate reliably. Thus, the combination of large values of both K_1 and k_1 in eq 6 resulted in experimental slopes which were rather small and insensitive to changes in methylarene concentrations. In other words the second term on the right side of eq 6 was minor. Accordingly, the second-order rate constant k_2 for mercuration was evaluated directly from the experimental rate constant k_{obsd} at each methylarene concentration as an average of at least five points. The listed values of k_2 in Table III are estimated to be reliable to within $\pm 20\%$. The rate constants were unaffected by the addition of lithium trifluoroacetate up to 0.01 M.

The overall reliability of the rate constants for arene mercuration are evaluated in Figure 6 by comparing the values obtained in dichloromethane with those in trifluoroacetic acid. The consolidated data in Table IV encompass the range of arenes from the electron-rich pentamethylbenzene to chlorobenzene at the other extreme and include the rate constants reported earlier by Olah, Fukuzumi, and co-workers.^{14,17,33} The linear free-energy relationship spans more than 5 orders of magnitude in reactivities, with a least-squares slope of 1.03 and a correlation coefficient of 0.98. We thus conclude that the solvent effect on arene activation during mercuration is the same in dichloromethane and trifluoroacetic acid despite a 30–50-fold increase in rate.

III. Thallium(III) Trifluoroacetate as an Electron Acceptor in π -Complex Formation. Spectrophotometric analysis established that various electron-rich methylarenes such as hexamethylbenzene, pentamethylbenzene, and tetra- and trimethylbenzenes form π -complexes with thallium(III) trifluoroacetate only after ionic dissociation,¹⁵ i.e., Scheme II. Quantitative measurements

Scheme II



established the monocation $Ti(O_2CCF_3)_2^+$ as the electron acceptor in π -complex formation. Thus, the CT absorbance in this system varied with the concentration of lithium trifluoroacetate in accord with the relevant Benesi-Hildebrand formulation for Scheme II, viz.,¹⁵ eq 9.

$$\frac{[Ti(O_2CCF_3)_3]}{A_{CT}} = \frac{1}{\epsilon_{CT}} + \frac{K_2 + [LiO_2CCF_3]}{K_2 K_3 \epsilon_{CT} [ArH]} \quad (9)$$

(33) A correction is included for an error in the measurement of the reactivity of 1,3,5-trimethylbenzene relative to 1,3-xylene of 13 rather than 157 reported in ref 14. Furthermore, we found the relative reactivities of 1,2,3-trimethylbenzene/1,3-xylene to be 1.9 and 1,2,4-trimethylbenzene/1,3-xylene to be 1.6, which compare with the reported values of 55 and 2.8, respectively.

Table V. Observed CT Absorption Bands of Aromatic Hydrocarbons with Thallium(III) Trifluoroacetate

arene	λ_{CT} , ^b nm	arene	λ_{CT} , ^b nm
hexamethylbenzene	364	1,2-xylene	330
hexaethylbenzene	366	1,3-xylene	326
pentamethylbenzene	343	1,4-xylene	311
1,2,3,4-tetramethylbenzene	342	<i>tert</i> -butylbenzene	330
1,2,3,5-tetramethylbenzene	332	isopropylbenzene	330
1,2,4,5-tetramethylbenzene	327	ethylbenzene	327
1,2,3-trimethylbenzene	337	toluene	324
1,2,4-trimethylbenzene	326	benzene	313
1,3,5-trimethylbenzene	327		

^aIn trifluoroacetic acid solution at 25 °C from ref 15. ^bCharge-transfer band (maximum).

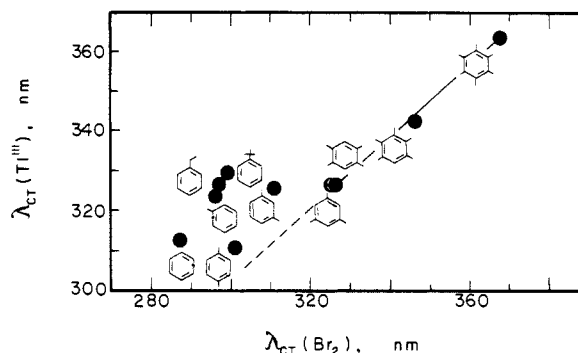


Figure 7. Comparison of the observed CT bands from thallium(III) trifluoroacetate with various arenes in trifluoroacetic acid with the corresponding CT bands from bromine. The line is arbitrarily drawn with a unit slope (see text).

In common with the results obtained with the isoelectronic acceptor $Hg(O_2CCF_3)_2$ in Figure 1, the CT band of these $Tl(O_2CCF_3)_2^+$ complexes shifted progressively to lower energies with the decrease in the ionization potential of the aromatic donors (see Table V). However, when the series was extended to the dimethylbenzenes and toluene, as well as to other monoalkylbenzenes which are relevant to this mechanistic study, we observed inconsistencies in the expected positions of the CT bands. This is illustrated in Figure 7, in which the values of $h\nu_{CT}$ for the $Tl(III)$ complexes are plotted against those for the well-known bromine complexes with the same series of arenes. The series of electron-rich methylarenes from hexamethylbenzene through to mesitylene show strikingly similar CT behavior for the $Tl(O_2CCF_3)_2^+$ and Br_2 acceptors, as indicated by fit to the line drawn with unit slope in Figure 7. On the other hand, the CT bands for $Tl(O_2CCF_3)_2^+$ complexes of the di- and monoalkylbenzenes are all shifted significantly to lower energies relative to the corresponding Br_2 complexes. Furthermore, the intensities of these CT bands were considerably weaker than those observed for mesitylene at the same concentrations. In order to test whether Scheme II was still applicable to these less electron-rich arenes, we applied the Benesi-Hildebrand treatment given in eq 9 to toluene. A plot of absorbance change with lithium trifluoroacetate in Figure 8a does not support $Tl(O_2CCF_3)_2^+$ as the electron

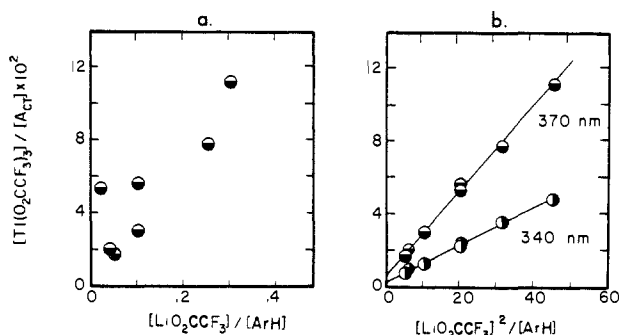


Figure 8. Typical Benesi-Hildebrand plots of the CT absorbances from thallium(III) trifluoroacetate and toluene according to (a) eq 9 and (b) eq 12 (the latter at the two monitoring wavelengths of 370 and 340 nm).

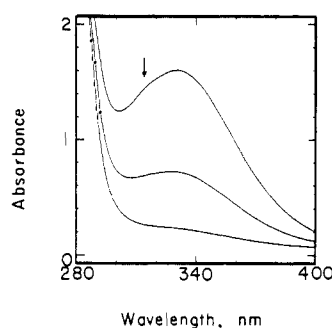
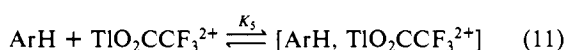


Figure 9. CT absorption spectrum from 0.01 M thallium(III) acetate and 0.01 M *tert*-butylbenzene with added lithium trifluoroacetate (top to bottom): 5.0×10^{-3} , 7.5×10^{-3} , and 1×10^{-2} M in trifluoroacetic acid at -20°C .

acceptor. Therefore a second scheme was formulated in which the dication was considered, i.e., Scheme III. The modified

Scheme III



Benesi-Hildebrand relationship for this species is eq 12. Indeed the plot of the absorbance change with $[\text{LiO}_2\text{CCF}_3]^2$ in Figure 8b followed this relationship under conditions in which $K_4 \ll [\text{LiO}_2\text{CCF}_3]^2$.

$$\frac{[\text{Ti}(\text{O}_2\text{CCF}_3)_3]}{A_{\text{CT}}} = \frac{1}{\epsilon_{\text{CT}}} + \frac{K_4 + [\text{LiO}_2\text{CCF}_3]^2}{K_4 K_5 \epsilon_{\text{CT}} [\text{ArH}]} \quad (12)$$

Furthermore, the CT absorbance was considerably more sensitive to $[\text{LiO}_2\text{CCF}_3]$ than that observed for hexamethylbenzene (eq 9), in accord with the second-order dependence of the trifluoroacetate concentration in eq 12. The preequilibrium and association constant term $K_4 K_5$ was evaluated as $2.5 \pm 0.3 \times 10^{-4}$ M at $\lambda = 340$ and 370 nm with $\epsilon_{\text{CT}} = 431$ and $159 \text{ M}^{-1} \text{ cm}^{-1}$, respectively, for the dicationic π -complex.

We conclude from these studies that thallium(III) trifluoroacetate forms two types of π -complexes as a result of the ionic dissociation of one and two trifluoroacetate ligands. Electron-rich arenes interact preferentially with the monocation (Scheme II), whereas the less endowed members interact with the dication (Scheme III), which is also expected to be a stronger acceptor. Indeed a close inspection of the CT absorption spectrum of the π -complex with *tert*-butylbenzene in Figure 9 reveals a high-energy shoulder at $\lambda \sim 315$ nm, which may be taken as a minor contribution of the π -complex from the monocation.

IV. Rates of Arene Thallation with Thallium(III) Trifluoroacetate. Kinetics analysis established the active electrophile in the thallation of hexamethylbenzene, pentamethylbenzene, and the various tetra- and trimethylbenzenes to be the monocation

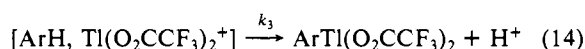
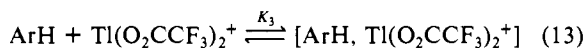
Table VI. Relative Reactivities of Arenes Toward Thallation in Trifluoroacetic Acid^a

substituted benzene	k_{rel}^b	substituted benzene	k_{rel}^b
pentamethyl	86 400	1,4-dimethyl	110
1,2,4,5-tetramethyl	3 700	1,2-dimethyl	850
1,2,3,5-tetramethyl	37 600	<i>tert</i> -butyl	88
1,2,3,4-tetramethyl	44 000	isopropyl	74
1,2,3-trimethyl	9 300	ethyl	70
1,2,4-trimethyl	5 800	methyl	62
1,3,5-trimethyl	16 200	none	1.0
1,3-dimethyl	1 500	chloro	0.03

^a At 25°C . ^b Second-order rate constant evaluated relative to that of benzene.

$\text{Ti}(\text{O}_2\text{CCF}_3)_2^+$, which is the same species involved in π -complex formation¹⁵ (Scheme IV). The variation in the trifluoroacetate

Scheme IV



concentration with the aid of lithium trifluoroacetate provided the experimental means to establish the kinetics for Scheme IV, i.e., eq 15.

$$\frac{1}{k_{\text{obsd}}} = \frac{1}{k_3} + \frac{[\text{LiO}_2\text{CCF}_3]}{k_3 K_2 K_3 [\text{ArH}]} \quad (15)$$

However under these conditions, the CT absorption bands of the π -complexes derived from the less electron-rich mono- and dialkylbenzenes were too weak to be measured. (Moreover the CT spectra observed at higher concentrations of Tl(III) were associated with a different series of dicationic complexes $[\text{ArH}, \text{TiO}_2\text{CCF}_3^{2+}]$, as depicted in Figure 8.) Since we could not reliably extend the spectrophotometric method to these arenes, we determined their relative reactivities by the competition method.³⁴ Thallium(III) trifluoroacetate and LiO_2CCF_3 in trifluoroacetic acid was treated with a molar excess (>10 -fold) of a mixture containing pairs of arenes, and the reaction was then quenched with sodium iodide.^{4c} The corresponding mixtures of aryl iodides were identified by GC/MS analysis in comparison with authentic samples and quantitatively determined by gas chromatography using the internal standard method (see Experimental Section). The same results were obtained from an alternative analytical procedure based on the prior isolation of the arylthallium dichlorides followed by brominolysis to the corresponding mixture of aryl bromides.¹⁴

The relative reactivities of the arenes in Table VI were determined either by direct kinetics measurements (electron-rich arenes) or by the competition method. The reliability of the two procedures was evaluated with mesitylene and pseudocumene—the relative reactivity $k_{\text{M}}/k_{\text{P}} = 2.7$ from kinetics¹⁵ and 2.9 by competition. The results of the competition method are also cross-checked with several arene pairs. For example, the relative reactivity of *o*-xylene and toluene was $k_{\text{X}}/k_{\text{T}} = 12$ by direct competition and 13 by an indirect competition based on *m*-xylene/toluene (25) and *o*-xylene/*m*-xylene (0.52) pairs. Analogously the relative reactivity of mesitylene and toluene $k_{\text{M}}/k_{\text{T}} = 2.4 \times 10^2$ was obtained from the indirect competition involving toluene/*o*-xylene/mesitylene pairs which compares with 2.5×10^2 based on toluene/*m*-xylene/pseudocumene/mesitylene pairs.

It is especially important that the relative reactivities of the less substituted benzenes be based on the competition method, since this procedure minimizes any ambiguity which could arise from the multiple dissociation of thallium(III) trifluoroacetate (see Figure 8). Such complications are undoubtedly inherent in the discrepancy of the rate constants for thallation (especially in

(34) See similar competition experiments in ref 4c, 9, and 12b.

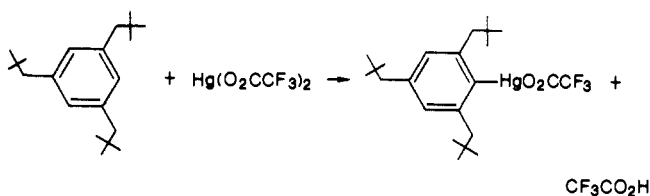
Table VII. Steric Effects on π -Complex Formation and Rates of Mercuration and Thallation of 1,3,5-Trialkylbenzenes^a

$R_3C_6H_3$ alkyl (R)	IP, ^b ev	thallation			mercuration		
		λ , ^c nm	K_3 ^d	k_2 , ^e $M^{-1} s^{-1}$	λ , ^c nm	K_1 , ^f M^{-1}	k_2 , ^e $M^{-1} s^{-1}$
methyl	8.40	327	130	56	345	28	31
ethyl	8.32	331	250				
isopropyl	8.24	330	430	12	330	180	26
neopentyl	8.19	344	200	<0.1	350	140	0.16
<i>tert</i> -butyl	8.19	339	42	<0.1	340	96	0

^a In trifluoroacetic acid at 25 °C. ^b Vertical ionization potential of the uncomplexed arene. ^c Wavelength for monitoring the CT absorbance. ^d Association constant in eq 8. ^e Overall second-order rate constant evaluated kK_3 .³² ^f Association constant in eq 1.

the absence of added lithium trifluoroacetate) as previously measured by visible spectrophotometry and NMR integration.³⁵ Similarly we find that toluene and mesitylene are roughly comparable when their reactivities were evaluated spectrophotometrically from the disappearance of the CT absorption bands derived from thallium(III) trifluoroacetate, especially in the absence of added lithium trifluoroacetate. By contrast, competition experiments carried out under the same conditions clearly established mesitylene to be 260 times more reactive than toluene, as listed in Table VI.

V. Steric Effects in π -Complex Formation and Rates of Mercuration and Thallation. The series of 1,3,5-trialkylbenzenes with increasing size of the alkyl substituent were investigated as a further basis for the comparison of mercuration and thallation. The association constants of the arenes ranging from mesitylene to the highly encumbered trineopentyl and tri-*tert*-butylbenzenes were determined and the second-order rate constants for thallation and mercuration evaluated by the procedures described above. The magnitudes of the rate constants in Table VII indicate minimal differences in steric effects for mesitylene, triethylbenzene, and triisopropylbenzene. Extending the series to trineopentylbenzene leads to a sharp falloff in the rates of both thallation and mercuration. Since only a minor steric effect is observed in the association constants, the decrease in the overall reaction rate for trineopentylbenzene can be attributed to the rate-limiting collapse of the π -complex. Owing to the rather slow rates of mercuration of trineopentylbenzene, we made repeated attempts to isolate single crystals of the π -complex. However, we were able only to isolate the mercuration product,



the ORTEP diagram of the X-ray crystal structure of which is shown in Figure 10. Similarly, trineopentylbenzene reacted with thallium(III) trifluoroacetate in trifluoroacetic acid to the corresponding thallated product which was characterized as the 2,4,6-trineopentylthalliodobenzene derivative after iodide cleavage.

Mercuration and thallation are somewhat differentiated in the sterically hindered tri-*tert*-butylbenzene. Thus, the exposure to mercury(II) trifluoroacetate in trifluoroacetic acid leads to no change in the CT spectrum over the course of several hours. Evaluation of the π -complex formation according to eq 2 for Scheme I leads to an association constant of $K_1 = 96 M^{-1}$ ($\epsilon_{CT} = 1700 M^{-1} cm^{-1}$ at 340 nm) which is in line with those measured for the triethyl and triisopropyl analogues. Thus, steric hindrance plays a dominant role only in the collapse of the π -complex.

Under the same conditions tri-*tert*-butylbenzene reacted with thallium(III) trifluoroacetate over a period of 12 h, as judged by the slow disappearance of the CT absorbance. Attempts to measure the association constant K_3 of tri-*tert*-butylbenzene with thallium(III) trifluoroacetate with the aid of the Benesi-Hilde-

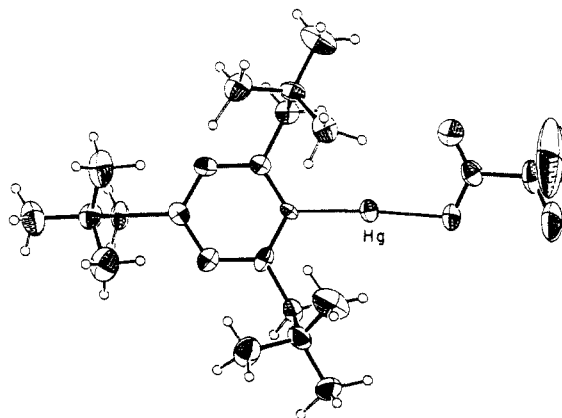


Figure 10. ORTEP diagram of 2,4,6-trineopentylphenylmercury(II) trifluoroacetate from the mercuration of 1,3,5-trineopentylbenzene showing the 2- and 6-neopentyl groups above the aromatic plane and the 4-neopentyl group below.

brand method gave ambiguous results. For example, spectrophotometric analysis of the CT absorbances at various concentrations of lithium trifluoroacetate partially followed the trend in eq 9 and 12 for the formulations in Scheme II and III, respectively. We suspect that a mixture of π -complexes derived from both $Tl(O_2CCF_3)_2^+$ and $TlO_2CCF_3^{2+}$ were extant, although we saw no evidence of a composite band in the CT absorption spectrum (compare Figure 9). The spectral maximum of $\lambda_{CT} = 339$ nm is close to that at 343 nm in the trineopentylbenzene complex which does follow the behavior in eq 9 expected for the $Tl(O_2CCF_3)_2^+$ complex. The mixture of products reflects a similar dichotomy in the interaction of thallium(III) trifluoroacetate with tri-*tert*-butylbenzene. Thus, at least three major products were separated by gas chromatography after quenching the reaction mixture with iodide. Two of them were identified by GC/MS analysis as the dealkylation product 1,3-di-*tert*-butylbenzene and the cleavage product 3,5-di-*tert*-butyliodobenzene in low yields. Since we could find no evidence for 2,4,6-tri-*tert*-butyliodobenzene, we conclude that no aromatic thallation occurred.

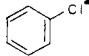
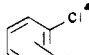
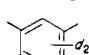
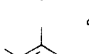
VI. Kinetic Isotope Effects for Mercuration and Thallation.

The rates of mercuration of the ring-deuteriated mesitylene- d_3 , durene- d_2 , and pentamethylbenzene- d_1 were measured in dichloromethane. A comparison of the association constants for various arenes determined by the kinetics procedure (Table II) with the deuteriated analogues in Table VIII indicate no equilibrium isotope effect in π -complex formation. The same results were obtained from independent measurements of K_1 by the Benesi-Hildebrand method. By contrast, the rates of mercuration of these arenes show sizable kinetic isotope effects. (See column 4, Table VIII.) It is noteworthy that the magnitudes of the kinetic isotope effect for the mercuration of durene and pentamethylbenzene are somewhat larger than the isotope effects observed during the side-chain substitution of a methyl group as it was induced by $Tl(III)$. No side-chain substitution occurred during the mercuration of any of the methylbenzenes. The kinetic isotope effects for thallation of pentamethylbenzene and durene of $k_H/k_D = 2.6$ and 2.5, respectively, were included in the earlier study.¹⁵

The kinetic isotope effect for the mercuration of chlorobenzene was determined by two procedures. The kinetic method was

(35) (a) Roberts, R. M. G. *Tetrahedron* **1980**, *36*, 3281. (b) Al-Azzawi, S. F.; Roberts, R. M. G. *J. Chem. Soc., Perkin Trans. 2* **1982**, 677.

Table VIII. Kinetic Isotope Effects for the Mercuration of Various Arenes

	K_1 , M ⁻¹	k_1 , s ⁻¹	k_H/k_D
	1.1	2.0	
	1.2	0.52	3.8 (3.9) ^b
	8.7 (6.9) ^c	0.20	4.7 ^d
	13 (13) ^e	1.6	5.4 ^d

^a Measured in trifluoroacetic acid at 60 °C by the CT method.

^b Measured in trifluoroacetic acid at 25 °C by competition method.

^c Under the same conditions as those in Table II. ^d Calculated from column 3 and Table II, column 4. ^e Measured spectroscopically by the Benesi-Hildebrand method.

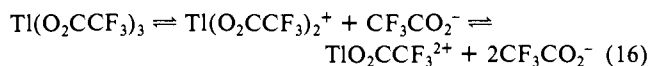
examined with chlorobenzene and chlorobenzene-*d*₅ at 60 °C to achieve reasonable rates according to eq 6. To circumvent any ambiguity in the measurements at these temperatures, we also carried out a competition between chlorobenzene and chlorobenzene-*d*₅ at 25 °C. Mass spectral analysis of the arene base peaks at *m/z* 112 and 117 afforded the kinetic isotope effects of 3.9 ± 0.1 at 10% and 30% conversions.

Discussion

Mercuration and thallation represent the activation of arenes by the substitution of a nuclear hydrogen with a reactive metal electrophile, such as mercury(II) and thallium(III) trifluoroacetates examined in this study. Kinetic studies have established the principal active forms of the electrophile in mercuration and thallation to be the neutral $\text{Hg}(\text{O}_2\text{CCF}_3)_2$ and the cationic $\text{Tl}(\text{O}_2\text{CCF}_3)_2^+$, respectively. Thus, the ionic dissociation of mercury(II) trifluoroacetate to the cation as depicted in eq 3 is not important. On the other hand, the neutral form of thallium(III)



trifluoroacetate is an inactive electrophile. As such, thallation requires prior dissociation primarily to the monocation for activation even in the nonpolar dichloromethane ($\epsilon_{\text{CH}_2\text{Cl}_2} = 9.08$). The second dissociation to the dication can also be relevant (See Figure 8).



Although the active electrophiles $\text{Hg}(\text{O}_2\text{CCF}_3)_2$ and $\text{Tl}(\text{O}_2\text{CCF}_3)_2^+$ are isoelectronic (and probably isostructural)^{36,37} species, they basically differ in the charge they bear. Accordingly, the activation processes for mercuration and thallation show strong similarities, and at the same time they exhibit some striking differences. We thus wish to take this opportunity to delineate the mechanistic features inherent to arene activation by a quantitative comparison of this pair of related electrophiles.

I. π -Complexes as Intermediates in Mercuration and Thallation. Comparison of Their Ground and Excited States. Quantitative spectrophotometric analyses have established the transient charge-transfer absorption spectra observed during mercuration and thallation to derive from the same electrophilic species involved in the kinetics, viz., $\text{Hg}(\text{O}_2\text{CCF}_3)_2$ and $\text{Tl}(\text{O}_2\text{CCF}_3)_2^+$, respectively. Indeed these species form two series of arene π -complexes $[\text{ArH}$,

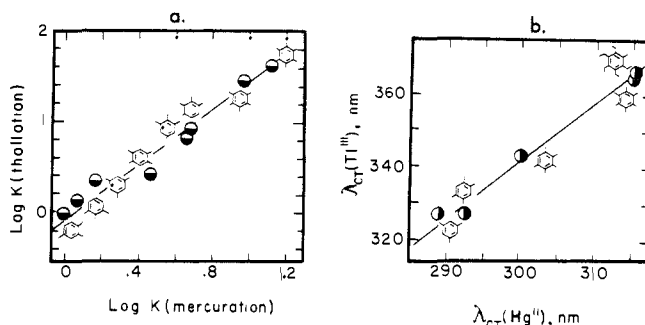
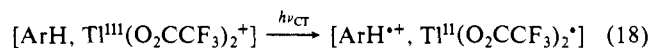
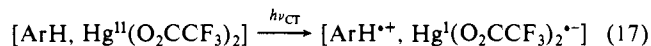


Figure 11. Ground-state and excited-state similarities of the π -complexes of mercury(II) and thallium(III), as shown by (a) association constants (K) and (b) CT absorption spectra (λ_{CT}).

$\text{Hg}(\text{O}_2\text{CCF}_3)_2$] and $[\text{ArH}, \text{Tl}(\text{O}_2\text{CCF}_3)_2^+]^+$ which bear strong resemblances to each other, both in the ground state and in the CT excited state.³⁸

(a) **Ground-State** similarities of the mercury(II) and thallium(III) π -complexes are reflected in the linear relationship of the association constants ($\log K$) in Figure 11a, which indicates that the stabilization of both series of π -complexes is affected in the same way with changes in the arene structure. The correlation with a slope of 1.4 indicates that the cationic complexes $[\text{ArH}, \text{Tl}(\text{O}_2\text{CCF}_3)_2^+]^+$ are stabilized about 40% more than their neutral counterparts $[\text{ArH}, \text{Hg}(\text{O}_2\text{CCF}_3)_2]$.⁴⁰

(b) **CT excited state** similarities of the arene complexes of $\text{Hg}(\text{O}_2\text{CCF}_3)_2$ and $\text{Tl}(\text{O}_2\text{CCF}_3)_2^+$ are revealed in the parallel trend in their absorption bands in Figure 11b.⁴⁰ Thus, for weak electron donor-acceptor complexes of the type described as π -complexes,¹⁶ the spectral transition $h\nu_{\text{CT}}$ represents an electronic excitation of the arene moiety from the neutral ground state to the polar excited state, i.e., its photoionization to an electrophilic acceptor.³¹ For the mercury(II) complexes, the relevant CT transition corresponds to eq 17, and for the thallium(III) complexes, it is eq 18. Both



series of π -complexes share the arene cation in the form of the radical pair shown in the brackets in the equations as the CT excited state according to expectations of Mulliken theory.^{18,19} The slope of 1.3 in the linear correlation (Figure 11b) indicates that the energy of the CT excitation of the cationic π -complex from $\text{Tl}(\text{O}_2\text{CCF}_3)_2^+$ is merely $\sim 30\%$ more sensitive to changes in arene structure compared to that derived from $\text{Hg}(\text{O}_2\text{CCF}_3)_2$.⁴⁰ Otherwise, both series of π -complexes show parallel behavior in the transformation to the CT excited state.

The similarity in the π -complexes of $\text{Hg}(\text{O}_2\text{CCF}_3)_2$ and $\text{Tl}(\text{O}_2\text{CCF}_3)_2^+$ with the series of sterically crowded 1,3,5-trialkylbenzenes as listed in Table VII indicates that the CT interaction occurs at relatively long range. The latter was confirmed by the

(38) (a) The mercury(II) arene complexes are to be distinguished from the arene-mercurium ions found in superacid media.³⁹ Compare ref 29 and: (b) Sokolov, V. I.; Bashilov, V. V.; Reutov, O. A. *Dokl. Akad. Nauk SSR* **1971**, *197*, 101.

(39) (a) Olah, G. A.; Yu, S. H.; Parker, D. G. *J. Org. Chem.* **1976**, *41*, 1983. (b) Damude, L. C.; Dean, P. A. W. *J. Organomet. Chem.* **1979**, 1811. (c) We find that when hexamethylbenzene is mixed with an equimolar amount of the cationic mercury(II) salt $\text{Hg}(\text{SbF}_6)_2$ in dichloromethane at 25 °C, a pair of new absorption bands appear at $\lambda_{\text{max}} = 293$ and 406 nm. This spectrum is attributed to the σ -complex hexamethylmercuribenzenium ion in comparison with that of the heptamethylbenzenium ion.²⁹ At low temperatures its appearance is preceded by the CT bands of the EDA complex. [We thank Dr. P. A. W. Dean for a generous sample of $\text{Hg}(\text{SbF}_6)_2$.] When hexamethylbenzene is treated with $\text{Hg}(\text{O}_2\text{CCF}_3)_2$ under the same conditions (or in trifluoroacetic acid), only the CT bands are observed (see Figure 1). The concentration of the corresponding π -complex is clearly too low to observe with $\text{Hg}(\text{O}_2\text{CCF}_3)_2$ owing to its weaker acceptor properties compared to $\text{Hg}(\text{SbF}_6)_2$.

(40) Note the correlation includes only the electron-rich arenes owing to complications from $\text{TlO}_2\text{CCF}_3^{2+}$ with the others. See Figures 7-9.

(36) Douglas, B. E.; McDaniel, D. H.; Alexander, J. T. *Concepts and Models of Inorganic Chemistry*, 2nd ed.; Wiley: New York, 1983; p 63.

(37) (a) Allman, R. Z. *Kristal.* **1973**, *138*, 366. (b) Barron, P. F. *J. Organomet. Chem.* **1982**, *236*, 157.

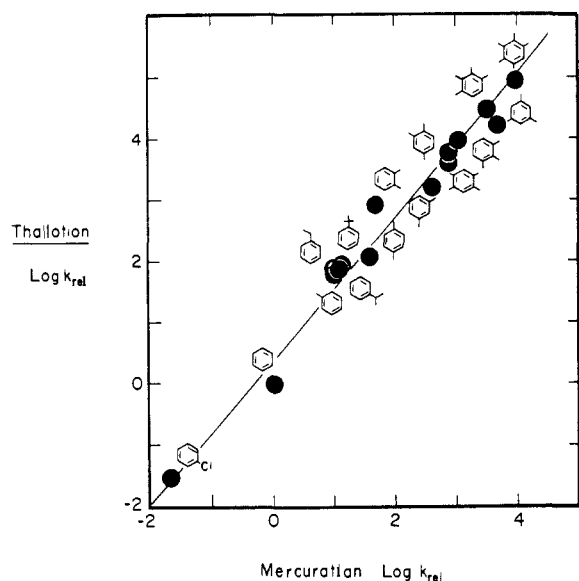


Figure 12. Direct relationship of the relative reactivities (k_{rel}) of arenes in mercuration and thallation.

pair of long Hg–C bond distances in the η^2 -bonding of the electrophilic mercury(II) to the hexamethylbenzene donor by X-ray crystallography.²⁰ As a result, we expect any minor difference which may exist in the steric properties of Hg(O₂CCF₃)₂ and Tl(O₂CCF₃)₂⁺ to be obscured in the π -complexes, both in the ground state and in the CT excited state.

II. Comparison of the Activation Barriers for Mercuration and Thallation. The kinetics studies in Figure 5 and Table II also establish the neutral Hg(O₂CCF₃)₂ and the cationic Tl(O₂CCF₃)₂⁺ to be the principal electrophiles in mercuration and thallation,¹⁵ respectively. The reactivity trends in the two types of metalations were quantitatively compared in this study with a graded series of arenes ranging from the electron-rich pentamethylbenzene at one end to the least reactive arene chlorobenzene at the other extreme.

The relative reactivity of an arene to electrophilic metalation is represented by the activation free-energy difference, eq 19 where k represents the second-order rate constant and the subscript r

$$\Delta G_r^{\ddagger} = -2.3RT \log k/k_0 \quad (19)$$

refers to changes relative to that of benzene (k_0) arbitrarily chosen as the reference arene (see Tables II and III). The direct comparison between mercuration and thallation is shown in Figure 12, in which the logarithms of the ratio of second-order rate constants for mercuration (Table II) are plotted against those for thallation in trifluoroacetic acid (Table VI). Although thallation rates could not be examined in dichloromethane, a similar linear correlation to that shown in Figure 12 is obtained for mercuration rates in dichloromethane with thallation rates in trifluoroacetic acid, as follows from the linear relationship illustrated in Figure 6. The striking linear free-energy correlation spans more than 6 decades in rate with a 1:1 relationship, as shown by the fit of the data to the line drawn with a slope of unity. In other words, *those factors relevant to surmounting the activation barrier for mercuration are mirrored in exactly the same way during thallation as a consequence of systematic changes in the arene donor.*

III. Correlation of the Rates of Mercuration and Thallation with the CT Excitation Energies of the π -Complexes. The relative reactivities of arenes to metalation are represented by the activation free-energy difference ΔG_r^{\ddagger} in eq 19. In the same way, the transition energy $h\nu_{CT}$ associated with the charge-transfer excitation of the π -complex can be evaluated from the absorption spectrum (λ_{CT}) by a similar comparative method, i.e., eq 20 where

$$\Delta h\nu_{CT} = h\nu_{CT} - h\nu_{CT}^0 \quad (20)$$

$h\nu_{CT}^0$ is the CT transition energy of the benzene π -complex.¹⁷ In

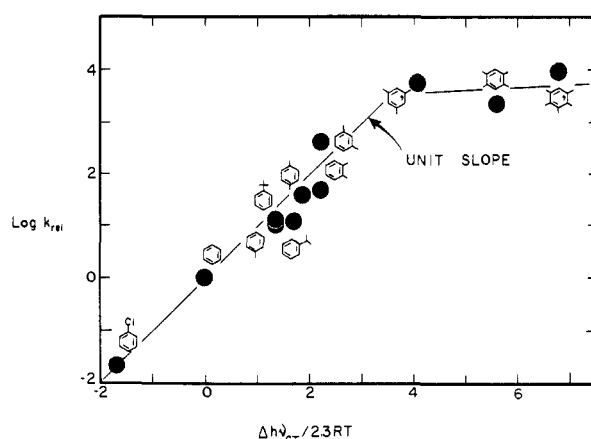


Figure 13. Correlation of the relative reactivities (k_{rel}) of arene in mercuration with the CT transition energy according to eq 20. The inclined line is arbitrarily drawn with a slope of unity.

the comparative method, the values of $\Delta h\nu_{CT}$ focus primarily on the contribution from the arene moiety since the electrophile component largely cancels out in the difference procedure.

The correlation of the activation barriers with the CT excitation energies shown in Figure 13 for mercury(II) clearly consists of two trends. At the low end of the reactivity scale (chlorobenzene to the xylenes), a linear plot is observed for the CT transition energy with a slope of close to unity. In other words, these mercuration rates relate to the CT excited state of the π -complex with a free-energy relationship described as in eq 21.

$$\log k/k_0 = -\Delta h\nu_{CT}/2.3RT + \text{constant} \quad (21)$$

On the other hand, the flat portion of the slope in Figure 13 represents the most reactive arenes (mesitylene to pentamethylbenzene), which indicates that they are all mercured at essentially the same rate, quite independent of the donor properties as reflected in the CT transition energy of the π -complex. This trend is also observed in the interaction of the same arenes with thallium(III) (see Tables V and VI).⁴¹

IV. Relevance of Arene Ions in Electrophilic Aromatic Substitution. The linear free-energy relationship as expressed by eq 21 relates the activation barrier ΔG^{\ddagger} for aromatic substitution directly to the CT transition energy $h\nu_{CT}$ of the π -complex. Since $h\nu_{CT}$ pertains to the energetics of the photoionizations in eq 17 and 18, the correlation suggests that these arene ion pairs are reasonable approximations to the transition state for mercuration and thallation.^{17,42} Such a conclusion derives from the kinetics and spectral experiments with the less electron-rich arenes from chlorobenzene to the isomeric xylenes in Figure 13. Moreover, the leveling of the rates proceeding from the electron-rich arenes from mesitylene to pentamethylbenzene can be reconciled with this formulation in the following way. Let us consider the generalized kinetics scheme which is associated with the arene ion pair. In Scheme V, the activation step for electrophilic substitution proceeds from the thermal conversion ($\log k_e$) to the arene ion pair, which is to be likened to the photoactivation of the π -complex in eq 17.⁴⁴ The substitution product determining process (k_s)

(41) Unfortunately the obscuration of the relevant CT bands precluded our extending the plot for Tl(O₂CCF₃)₂⁺ to the less electron-rich arenes from chlorobenzene to the xylenes.

(42) Note that the solvation term which connects the thermal (adiabatic) and photochemical (vertical) ion pairs¹⁷ have been shown to be constant with arene donors.⁴³

(43) Howell, J. O.; Goncalves, J. M.; Amatore, C.; Klasinc, L.; Wightman, R. M.; Kochi, J. K. *J. Am. Chem. Soc.* **1984**, *106*, 3968.

(44) (a) In this treatment, the arene ion pair is considered to be close in energy to the transition state. Compare Hammond's postulate. (Hammond, G. S. *J. Am. Chem. Soc.* **1955**, *77*, 334.) (b) For a comparative description of ion pairs derived by CT excitation and by thermal activation, see discussions in ref 14. Fukuzumi, S.; Wong, C. L.; Kochi, J. K. *J. Am. Chem. Soc.* **1980**, *102*, 2928. Klingler, R. J.; Fukuzumi, S.; Kochi, J. K. *ACS Symp. Ser.* **1983**, *211*, 117. (c) For the dissociative nature of the mercury(I) intermediate formed in eq 22, see ref 31.

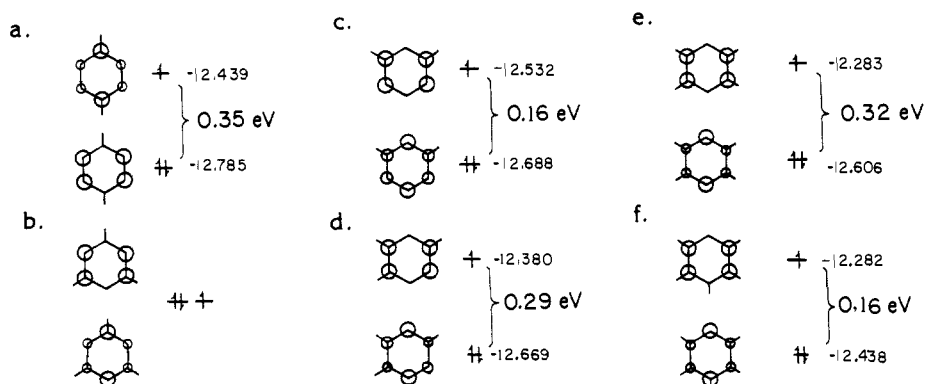


Figure 14. The symmetries and energies of the HOMO and SHOMO in the cation radicals of (a) *p*-xylene, (b) mesitylene, (c) *m*-xylene, (d) pseudocumene, (e) durene, and (f) pentamethylbenzene.

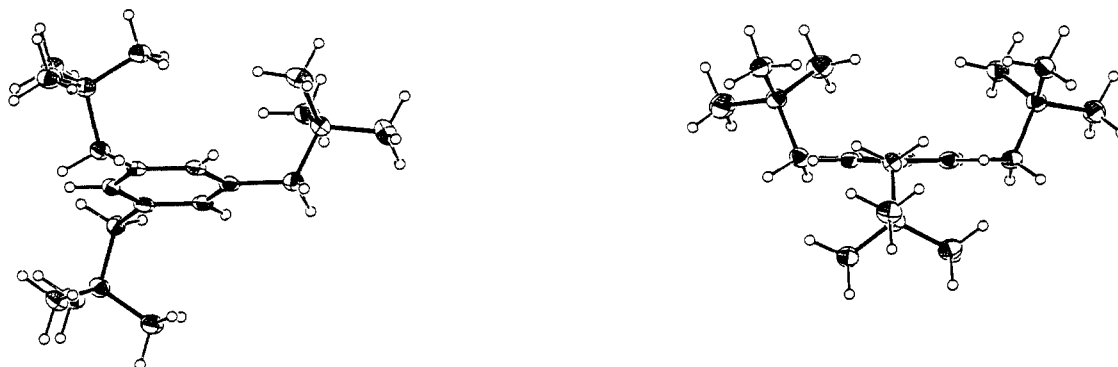
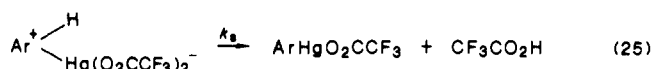
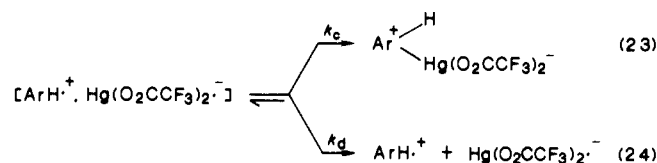
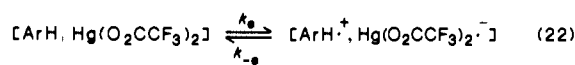


Figure 15. ORTEP drawings of 1,3,5-trieneopentylbenzene in three-quarters (left) and end (right) perspectives showing the dispositions of the neopentyl groups above and below the aromatic plane.

Scheme V

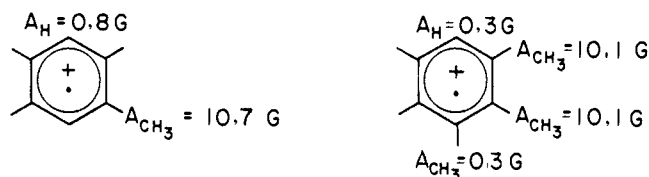


is then dependent on the rate constants k_c and k_d for collapse to the Wheland intermediate and diffusive separation to free ions, respectively. Since the rate constant k_d is likely to be invariant between a given electrophile and a series of structurally related arenes, the rate of aromatic substitution will be strongly mediated by the value of k_c . If for some reason the rate of arene ion pair collapse is retarded, the competition from back electron transfer (k_{-e}) will become increasingly important. Under these circumstances, the reaction rate will no longer follow the linear free-energy relationship in eq 21. Indeed at some point back electron transfer will dominate (i.e., $k_{-e} \gg k_c$), and it is conceivable that little or no thermal reaction will take place.⁴⁶

Let us now consider how the experimental variables pertaining to (a) electronic effects, (b) steric effects, (c) solvent effects, and (d) product studies can be reconciled with Scheme V in terms of the facility with which such an arene ion pair collapses.

(a) **Electronic effects** in the collapse of the arene ion pair can be viewed as the influence of substituents on the spin density in the singly occupied orbital (SOMO) requisite to bond formation

in eq 23. For example, in mesitylene the pair collapse at any of the three unsubstituted nuclear positions is unimpeded since the SOMO is degenerate (see Figure 14b). Similarly the SOMOs in the cations of *p*-xylene, *m*-xylene, and pseudocumene are conducive to pair collapse at the free positions owing to the available spin densities in Figure 14, parts a, c, and d, respectively. By contrast, the SOMOs of the cations of durene and pentamethylbenzene have nodes at the free 3- and 6-positions (parts e and f), and collapse there is not favored. Indeed the lack of spin density at these positions of durene and pentamethylbenzene cations, respectively, accords with the observed magnitudes of the ¹H hyperfine splittings in the ESR spectra,^{47,48} i.e.,



Thus, the pair collapse of durene and pentamethylbenzene cations is only favored at the already substituted ipso positions and is probably a reversible process. Alternatively, collapse at an unsubstituted position suffers from the promotional energy of 4–7 kcal mol⁻¹ from the subjacent orbital.⁴⁹ Such a retardation of the pair collapse of durene and pentamethylbenzene cations could account for the leveling effect depicted in Figure 13 and the attendant breakdown of the linear free-energy relationship.

Alternatively, it is possible to consider the latter as reflecting a change in the nature of the rate-determining step, as emphasized

(45) In this mechanism, the isomer distributions are determined in a step subsequent to the activation process. As such it provides the basis for understanding aromatic substitution patterns which allow low substrate reactivities but high regioselectivities. For further discussion see ref 17.

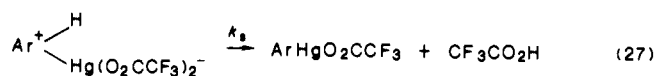
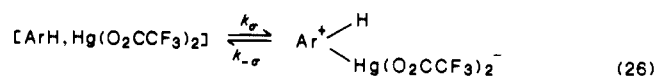
(46) Compare the absence of a thermal reaction of $\text{Hg}(\text{O}_2\text{CCF}_3)_2$ with hexamethylbenzene despite its low ionization potential.

(47) Dessau, R. M.; Shih, S.; Heiba, E. I. *J. Am. Chem. Soc.* **1970**, *92*, 412.

(48) Vincow, G. In *Radical Ions*; Kaiser, E. T., Kevan, L., Eds.; Wiley: New York, 1968.

(49) The orbital energies in Figure 14 were calculated by the extended Huckel molecular orbital method (Wang, D.-X., private communication).

Scheme VI

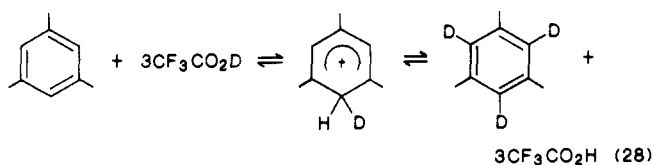


in an abbreviated formulation (Scheme VI). If the formation of the σ -complex were rate limiting, then $k_s \gg k_{-\sigma}$. Thus, the experimental rate constant is $k_{obsd} = k_{\sigma}$, and the linear free-energy relationship in eq 21 is applicable as described above. On the other hand, if the breakup of the σ -complex were rate limiting, then $k_s \ll k_{-\sigma}$. Thus, the experimental rate constant is $k_{obsd} = k_s - (k_{\sigma}/k_{-\sigma})$, and the rate of proton transfer from the σ -complex is relatively slow. This situation may well lead to the observed leveling in Figure 13 as a result of compensating effects on the preequilibrium ($k_{\sigma}/k_{-\sigma}$) and deprotonation rate (k_s) in durene and pentamethylbenzene.⁵⁰ However, the results in Table VIII indicate that the kinetic isotope effect for chlorobenzene is more or less the same as that for durene and pentamethylbenzene.⁵¹ Such an invariance of the kinetic isotope effect suggests that arene reactivity is not differentiated by the rate of proton loss from the σ -adduct. We therefore conclude that a change in the rate-limiting steps in Scheme V is alone insufficient to account for the leveling effect in Figure 13.

(b) **Steric effects** in mercuration and thallation are manifested by the substitution rate for trineopentylbenzene which is more than 2 decades slower than that for mesitylene, despite their similar donor properties. Indeed the molecular structure of trineopentylbenzene shown in the ORTEP perspectives in Figure 15 emphasizes the extent to which both of its faces are protected—the neopentyl substituents extending reasonably far above and below the aromatic plane.⁵² Also, a dynamic equilibration of these bulky groups is expected in solution. Since the association constants and CT transition energies are comparable for trineopentylbenzene and mesitylene (Table VII), the steric effects extant in the π -complexes and in the arene ion pairs are not sufficient to account for the observed rate difference. This conclusion is also in accord with the long-range interaction observed in the X-ray structure of the crystalline complex.²⁰ Therefore, steric effects according to Scheme V arise during arene ion pair collapse. In the molecular structure of the mercured trineopentylbenzene, the heteroatom substituent occupies a position on the side opposite the aromatic ring from the pair of neighboring neopentyl groups (see Figure 10). Thus, in order for pair collapse to the σ -adduct or Wheland intermediate to occur, a substantial steric barrier must be overcome to obtain a structural configuration akin to the product.

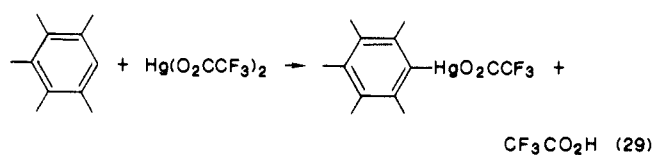
Steric inhibition of aromatic substitution is even more severe in 1,3,5-tri-*tert*-butylbenzene. Although the formation of the π -complex with mercury(II) and thallium(III) is comparable to that of mesitylene (see Table VII), the persistence of the yellow CT bands indicated that little or no thermal reaction occurred.^{51b} The difficulty of attaining the σ -adduct of tri-*tert*-butylbenzene is also indicated in proton-exchange studies. Thus, mesitylene, durene, and even pentamethylbenzene undergo efficient proton exchange in trifluoroacetic acid via an analogous intermediate,¹⁵

e.g., eq 28. Under the same experimental conditions, no proton exchange was observed in 1,3,5-tri-*tert*-butylbenzene.

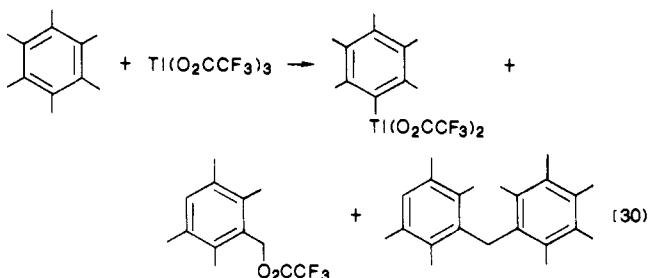


(c) **Solvent effects** in the pair collapse arises from charge stabilization by solvents with dielectric constants as different as trifluoroacetic acid and dichloromethane examined in this study (vide supra). The rates of arene mercuration are greatly increased in trifluoroacetic acid relative to those in dichloromethane—the enhancement factor being 30- to 50-fold in the second-order rate constants.⁵³ However, the *relative reactivity of a series of arenes is singularly unaffected by such a change in solvent* (see Figure 6). It is noteworthy that the arene ion radical pair when taken as a model for the transition state of aromatic substitution does correctly account for this otherwise inexplicable lack of solvent sensitivity on the relative reactivities of various arenes, despite the marked differences in the absolute rates. According to Scheme V, the latter arises from the large changes in the solvation which are expected to accompany the formation of the arene ion radical pair in eq 22, since the solvation energy of the neutral precursor may be neglected in comparison with that of the ion pair.¹⁷ However, by the comparative procedure (eq 19 and 20) used to develop the linear free-energy relationship in eq 21, we need only to consider the relative changes in solvation of the arene cation owing to contributions from the electrophile moiety which largely drop out by cancellation. Since the solvation energy of a series of related arene cations is relatively constant,⁴³ it follows for eq 21 that the relative reactivities would be solvent independent. It is noteworthy that the latter is difficult to reconcile with reactivity changes resulting from variable transition-state structures.

(d) **Product studies** provide a divergent view of the arene ion pair collapse during mercuration and thallation. The dichotomy is most pronounced in pentamethylbenzene. Thus, the treatment of pentamethylbenzene with $Hg(O_2CCF_3)_2$ affords the substitution product pentamethylphenylmercury trifluoroacetate in high yields (eq 22). No transient intermediates other than the π -complex



were observed in either the UV-vis or ESR spectra. On the other hand, our previous study¹⁵ of the thallation of pentamethylbenzene indicated that only 26% occurred by nuclear substitution, the remainder being accounted for by side products resulting from side-chain substitution and dimer formation (eq 30). Such side



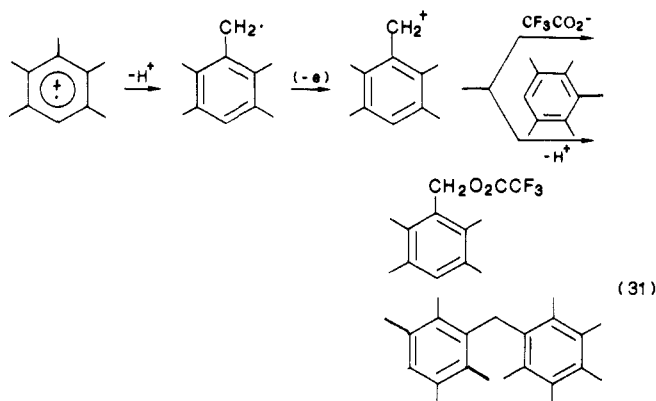
products are known to derive from the cation radical of pentamethylbenzene,⁵⁴ i.e., eq 31. Indeed the diversion to side products during thallation coincides with the direct observation of the arene

(50) The rates of formation (k_s) and decomposition ($k_{-\sigma}$) of the σ -complex are likely to respond to $h\nu_{CT}$ in opposite ways.

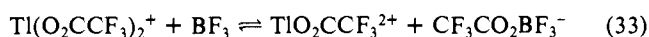
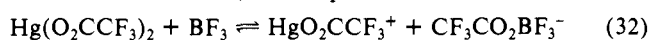
(51) (a) The same is true in thallation in which the kinetic isotope effect for chlorobenzene actually appears to be larger than that for either pentamethylbenzene or durene. (b) Analogously, thallium(III) trifluoroacetate reacted with tri-*tert*-butylbenzene only slowly but did not yield detectable amounts of substitution product (vide supra) owing to the difficulty in attaining the σ -intermediate.

(52) Note that the *syn, syn, anti* disposition of the trineopentyl groups in a crystal of 1,3,5-trineopentylbenzene differs from the all-*syn* conformation preferred for the 2,4,6-trihalo and trimethyl derivatives in solution, as determined by the temperature-dependent analysis of the 1H and ^{13}C NMR spectra. (Carter, R. E.; Nilsson, B.; Olsson, K. *J. Am. Chem. Soc.* **1975**, *97*, 6155.) The barrier for conformational interconversion is undoubtedly the lowest in 1,3,5-trineopentylbenzene. We thank Dr. A. Streitwieser for pointing out this previous study.

(53) Effects are readily apparent even when as little as a few percent of trifluoroacetic acid is present in dichloromethane. For the stabilizing effect of trifluoroacetic acid particularly of cations, see ref 28.



cation radical as a transient intermediate both by UV-vis and ESR spectroscopy.^{15,55} A similar dichotomy between the products of mercuration and thallation exists with durene, albeit to a lesser degree. Finally no discrepancy is observed with mesitylene, nuclear substitution occurring exclusively in both mercuration and thallation. Such a divergence between mercuration and thallation can be reconciled by the formulation in Scheme V if they differ by the extent to which diffusive separation (k_d) occurs in eq 24. All factors being the same, diffusive separation of the radical pair from mercury(II) should occur more readily than that from mercury(I) owing to a significant difference in the coulombic interactions—the arene ion being paired with the anionic $\text{Hg}^{\text{I}}(\text{O}_2\text{CCF}_3)_2^-$ in mercuration and with the neutral $\text{Tl}^{\text{III}}(\text{O}_2\text{CCF}_3)_2$ in thallation as illustrated in eq 17 and 18.⁵⁶ Moreover, the same electrostatic argument provides a ready rationalization for the ability of Lewis acids as additives to promote arene cation radical formation (leading to biaryls) during both mercuration and thallation of even unexceptional arenes.⁵⁷ Thus, the addition of boron trifluoride (as the etherate) will foster ionic dissociation of mercury(II) trifluoroacetate, i.e., eq 32 as well as thallium(III) trifluoroacetate cation,⁵⁸ i.e., eq 33. The results lead to a di-



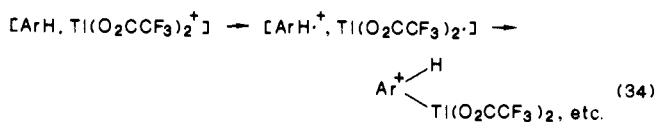
minution in the coulombic interaction in the radical pair $[\text{ArH}^{\bullet+}, \text{Hg}^{\text{I}}\text{O}_2\text{CCF}_3]$ during mercuration and enhancement of the coulombic repulsion in the radical pair $[\text{ArH}^{\bullet+}, \text{Tl}^{\text{III}}\text{O}_2\text{CCF}_3^+]$ during thallation. In both cases, the increased amounts of cage escape will lead to a higher component of electron-transfer derived products (such as biaryls). Attractive as such a simple electrostatic explanation may seem, cognizance must also be taken into account of the attendant change in the driving force for back electron transfer k_{-e} in eq 22. Unfortunately this factor cannot be evaluated at this point owing to the unavailability of the reduction potentials E° of these highly transient species.⁵⁹ Thus, the quantitative prediction of product yields derived from Scheme V must await the actual measurement of these quantities. Moreover the detailed solution of the kinetics including the isotope effects is likely to be even more complicated owing to rates which depend strongly on the various types of ion pairing which are likely to exist.⁶⁰ Finally we have thus far taken no cognizance of the spin mul-

tiplicity of the radical pairs in Scheme V. Our inability to observe CIDNP during arene mercuration or thallation unfortunately leaves unanswered the question of whether singlet-triplet interconversions play a role in mediating the individual rate constants for the CT formulation.

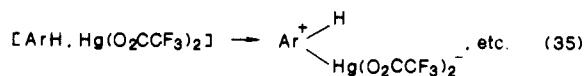
Summary and Conclusions

Stepwise and Concerted Mechanisms for Aromatic Substitution.

The study of mercuration and thallation has provided a sharp focus on the experimental delineation of stepwise and concerted mechanisms for arene activation. Thus, the unequivocal demonstration of arene cations as key intermediates in thallation, particularly of durene and pentamethylbenzene,¹⁵ is consistent with a stepwise (electron-transfer) mechanism for arene activation as in Scheme V,⁶¹ i.e., eq 34. By the same token, the singular



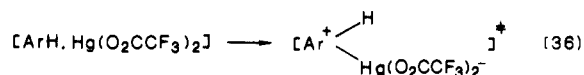
absence of any experimental evidence for such intermediates during mercuration is directly accommodated by a concerted (electrophilic) mechanism for arene activation, i.e., eq 35. The difficulty



with two separate mechanisms for arene activation by mercury(II) and thallium(III) is underscored by the striking correlation in Figure 12 which establishes the *activation barriers to follow identical trends*. In other words, the rate-determining processes for mercuration and thallation are similar, yet they distinctly differ in the products derived for the electron-rich arenes (durene and pentamethylbenzene in eq 31). Such a kinetics situation commonly demands that there exists at least one intermediate which separates the activation process from the products, as in Scheme V. This paradox can be resolved in one of two ways.

First, the mechanistic formulation in Scheme V merges stepwise and to concerted processes by the modulation of a pair of rate constants. According to Scheme V, the two principal pathways are differentiated during the competition between cage collapse (k_c) and diffusive separation (k_d) of the arene ion pair. The inability to observe the arene cation (e.g., from mesitylene) could be attributed to a rate of cage collapse to the Wheland intermediate occurring substantially faster than diffusive separation (i.e., $k_c \gg k_d$), which is tantamount to a concerted process. Likewise the ESR observation of the arene cation would derive from a diffusive process occurring faster than collapse (i.e., $k_c \ll k_d$), which could appear as a stepwise process. Some of the structural and environmental factors which influence both rate constants have been presented in the discussion above. However, this mechanism is not without its problems since it does not as yet address the observed kinetic isotope effects in a quantitative way (vide supra).

Second, the stepwise and concerted processes for arene activation may simply represent competing pathways, namely eq 36 and 37 where the superscript † represents the activated complex.



If so, those factors related to the donor properties of arenes, such as π -complex formation, CT excitation, activation barriers, etc.,

(54) For a review: Yoshida, K. *Electrooxidation in Organic Chemistry*; Wiley: New York, 1984.

(55) (a) Elson, I. H.; Kochi, J. K. *J. Am. Chem. Soc.* **1973**, *95*, 5060. (b) Sullivan, P. D.; Menger, E. M.; Reddoch, A. H.; Paskovich, D. H. *J. Phys. Chem.* **1978**, *82*, 1158.

(56) A similar electrostatic explanation can be used to account for the oxidative substitution of hexamethylbenzene by thallium(III) trifluoroacetate under conditions in which there is no reaction with mercury(II) trifluoroacetate.¹⁵

(57) McKillop, A.; Turrell, A. G.; Young, D. W.; Taylor, E. C. *J. Am. Chem. Soc.* **1980**, *102*, 6504.

(58) Preliminary studies of ionic dissociation of thallium(III) trifluoroacetate by changes in the ²⁰³Tl and ²⁰⁵Tl NMR spectra accompanying the addition of LiO₂CCF₃ qualitatively support eq 5. Quantitative measures of ionic dissociation by this method are pending. (Hinton, J. F., unpublished results.)

(59) For the metastable mercury(I) and thallium(II), see ref 31 and: (a) Cercek, B.; Ebert, M.; Shallow, A. J. *J. Chem. Soc. A* **1966**, 612. (b) Brown, D. M.; Dainton, F. S. *Trans. Faraday Soc.* **1966**, *62*, 1139.

(60) For a kinetics distinction between "intimate" (contact) and "solvent-separated" ion pairs, see: Lowry, T. H.; Richardson, K. S. *Mechanism and Theory in Organic Chemistry*; Harper and Row: New York, 1981; p 301 ff.

(61) (a) For related activations of arenes by electron transfer, see: Andrusis, P. J.; Dewar, M. J. S.; Dietz, R.; Hunt, R. L. *J. Am. Chem. Soc.* **1966**, *88*, 5483. Kochi, J. K.; Tang, R. T.; Bernath, J. *J. Am. Chem. Soc.* **1973**, *95*, 7114. (b) In the generalized formulation, each step in eq 34 is reversible (see Scheme V).

are too common to both to allow any distinction between these pathways. Moreover the common dependence on isoelectronic electrophiles, independent of charge, further obscures any difference in their transition states. This formulation thus recognizes two such dissimilar mechanisms as electron-transfer and electrophilic processes in mercuriation and thallation to be remarkably alike. Such kindred transition states can be theoretically accommodated within the valence bond approach to electrophile/nucleophile reactivity, as described by Shaik and Pross.⁶²

Crucial to the resolution of this dilemma is the understanding of the stepwise process for arene activation.⁶³ Particularly germane are the microdynamics of the "intimate" arene ion radical pairs in Scheme V, especially as they collapse or evolve to "loose" (solvent-separated) species and finally to "free" (separate) radical pairs. Indeed we have recently described in a related context how the CT excitation of π -complexes by a laser pulse provides access to arene ion radical pairs which can be examined directly by time-resolved spectroscopy.⁶⁴ Preliminary results with sterically hindered π -complexes such as 1,3,5-trineopentylbenzene-mercury(II) trifluoroacetate have yielded indications of arene cation radicals as intermediates. Hopefully further studies will provide the means to examine their fate in detail, especially with regard to spin multiplicity effects.

Experimental Section

Materials. The aromatic hydrocarbons were obtained from commercial sources and repurified as follows. Chlorobenzene, toluene, and *o*-, *m*-, and *p*-xylene (Matheson, Coleman and Bell) were refluxed over and distilled from sodium metal. 1,3,5-Tri-*tert*-butylbenzene (Aldrich Chemical Co.) was recrystallized from absolute ethanol and sublimed. 1,3,5-Triisopropylbenzene (Wiley Organics) and 1,3,5-trineopentylbenzene (as a gift from S. K. Chung) were used without further purification. *tert*-Butylbenzene and 1,3,5-triethylbenzene (Eastman) were distilled from sodium metal. 1-Chloro-5-iodobenzene (Aldrich) and *p*-iodotoluene (Pfaltz and Bauer) were used as received. Hexamethylbenzene, pentamethylbenzene, and durene (Aldrich) were recrystallized from ethanol and sublimed. Prehnitene and mesitylene (Aldrich) as well as isodurene and pseudocumene (Wiley Chemical Co.) were refluxed over sodium and distilled under reduced pressure. Hemimellitene (Aldrich) was converted to the crystalline sulfonic acid derivative which was purified and subsequently hydrolyzed.⁶⁵ The isomeric purity of each hydrocarbon was established by gas chromatographic analysis on a Hewlett-Packard 5790 chromatograph equipped with a 12-m capillary column coated with cross-linked methylsilicone.

Hexamethylbenzene- d_{18} (Merck) was received as a gift from Dr. A. E. Nader (Du Pont) and used as such. The ring deuteriated pentamethylbenzene- d_1 , durene-2,5- d_2 , and mesitylene-2,4,6- d_3 were prepared by proton exchange in trifluoroacetic acid. In a typical procedure, mesitylene (2.0 mL) was added to a mixture of trifluoroacetic anhydride (5 mL) and deuterium oxide (5 mL), and the solution was refluxed overnight. The reaction mixture was extracted with methylene chloride, and the extract was neutralized and dried with Na_2CO_3 . The solvent was removed in vacuo, and the mesitylene recovered after one exchange was 93%, as estimated by integration of the 1H NMR resonance of the aromatic proton relative to that of the methyl groups. The exchange procedure was repeated, and the recovered mesitylene upon distillation showed no aromatic protons (<1%) in the 1H NMR spectrum. The deuteriated mesitylene was further analyzed on a Hewlett-Packard Model 5992 gas chromatograph/mass spectrometer. The mass spectral cracking pattern of mesitylene- d_3 at 70 eV consisted of m/z (%) 108 (100), 122 (14), 123 (53), 124 (6), which was compared with that of mesitylene, 105 (100), 119 (10), 120 (42), 121 (4). Pentamethylbenzene- d_1 and durene- d_2 were prepared by a similar procedure. Each arene which was isolated after two exchanges was sublimed in vacuo and showed >99% deuteration of the aromatic protons. Chlorobenzene- d_5 was prepared by the chlorination of benzene- d_6 with $SbCl_5$.⁶⁶ In a typical procedure, antimony pentachloride (13.8 g) was added to 4.8 g of benzene- d_6 at -78

°C under an argon atmosphere. The frozen mixture was allowed to warm slowly to room temperature over a period of several hours. After stirring for 1 h at room temperature, the mixture of chlorobenzene and unreacted benzene- d_6 was distilled out of the crude reaction mixture. Fractionation afforded 2 g of chlorobenzene- d_5 . GC/MS analysis indicated >99% purity: m/z (%) 117 (100), 82 (60).

Thallium(III) trifluoroacetate was prepared from thallic oxide (AS-ARCO) as described previously.⁶⁷ Mercury(II) trifluoroacetate was prepared by a similar procedure from mercuric oxide and trifluoroacetic acid and recrystallized from a mixture of trifluoroacetic anhydride and trifluoroacetic acid.⁶⁸

Charge-Transfer Spectral Measurements. The UV-vis absorption spectra were measured on a Hewlett-Packard 8450A diode array spectrometer capable of 0.1-s time resolution and a repetition rate of 1 s. Temperature control of ± 0.1 °C was maintained by a Hewlett-Packard 89100 A thermostatic accessory. In a typical measurement, either a 10-, 2-, or 1-mm quartz cuvette equipped with side arm and Schlenk adaptor, was flame dried in vacuo and filled with dry argon. Aliquots (0.1–0.2 mL) of a solution of 0.01 M HgT_2 in either CH_2Cl_2 or CF_3CO_2H were transferred with the aid of airtight hypodermic syringes equipped with platinum needles to the main compartment under argon. An aliquot of 0.20 M arene dissolved in dichloromethane or trifluoroacetic acid (0.10 mL) was carefully loaded into the side arm by using the same technique. The cuvette was thermally equilibrated and the reaction initiated by a rapid shaking of the contents (<2 s).

The charge-transfer absorptions were measured at various concentrations of mercury(II) (typically $1-5 \times 10^{-3}$ M) and arenes (1×10^{-2} to 2×10^{-1} M), to ensure homogeneity in the band shapes and constancy of the maximum λ_{CT} . The spectra were measured repetitively at 2-s intervals, and the initial absorbance A_0 was obtained by extrapolation to zero time.¹⁵

Kinetics Measurements. The absolute rates of reaction between mercury(II) and the various arenes were followed spectrophotometrically by monitoring the disappearance of the charge-transfer absorption bands at selected wavelengths as indicated in the tables. The technique was essentially the same as that described above. Unless indicated otherwise, all the reactions were carried out in the dark at 25 °C, and their course followed to >90% completion. In a typical situation, aliquots of 0.01 M $Hg(O_2CCF_3)_2$ (0.20 mL) and 0.20 M arene (0.10 mL) in 1.5 mL of trifluoroacetic acid were employed. The pseudo-first-order rate constant k_{obsd} was obtained from the least-squares evaluation of the slope of the absorbance change $\ln(A_t - A_\infty)$ with time where A_t and A_∞ are the absorbances of the CT band at time t and final time, respectively. In all cases, linearity in the pseudo-first-order plots was attained with a correlation coefficient of 0.985 or better. The kinetics were carried out at various concentrations of the arenes. The relative rates of reaction of various arenes with $Hg(O_2CCF_3)_2$ were also determined by a competition method similar to that described by Olah, Stock, and co-workers.^{14,12}

The kinetic isotope effects were determined by measuring the individual rate constants spectrophotometrically for the normal arene and in a duplicate run for the deuteriated analogue. The mercuriations of toluene, chlorobenzene, and chlorobenzene- d_5 were determined at 60 °C to achieve reasonable rates. As a check, the kinetic isotope effect of chlorobenzene was also determined at 25 °C by the competition method. The relative amounts of chlorobenzene and chlorobenzene- d_5 consumed were determined by GC/MS analysis using the base peaks with m/z 112 and C_6D_5Cl (0.25 M in each) was prepared in trifluoroacetic acid. An aliquot of this mixture was washed with water, extracted with dichloromethane, and analyzed by GC/MS. After standing 12 h, another aliquot was worked up in a similar way. GC/MS analysis indicated the absence of proton exchange. For the competition experiment, mercury(II) trifluoroacetate was added and the mixture left in the dark. Aliquots were removed after 2 and 9 $\frac{1}{2}$ h and worked up as usual. GC/MS analysis of the recovered chlorobenzene indicated a kinetic isotope effect of 3.8 and 4.0 at 10% and 30% completion, respectively.

Product Identification and Analysis. All thermal reactions of arenes with mercury(II) trifluoroacetate were carried out in a Schlenk flask under an inert argon atmosphere and shielded from direct room light. Stock solutions of mercury trifluoroacetate (0.10 M) and the appropriate arene (0.10 M) were prepared in degassed trifluoroacetic acid (3.0 mL). When pentamethylbenzene and mercury(II) trifluoroacetate were mixed in equimolar amounts, mercuriation proceeded smoothly to pentamethylphenylmercury(II) trifluoroacetate [1H NMR: δ 2.25 (s, 6 H), 2.30 (s, 3 H), 2.54 (s, 6 H)] to consume all the pentamethylbenzene. Pentamethylphenylmercury(II) trifluoroacetate has been isolated in 83%

(62) (a) Shaik, S. S. *J. Am. Chem. Soc.* **1984**, *106*, 1227. (b) Pross, A.; Shaik, S. S. *Acc. Chem. Res.* **1983**, *16*, 363. (c) Pross, A. *Adv. Phys. Org. Chem.* **1985**, *21*, 99.

(63) Irrespective of stepwise and concerted mechanisms the linear free-energy correlation expressed in eq 21 emphasizes that the formation of the arene cation radical pair as in eq 22 is a suitable model for the activated complex in arene activation.¹⁷

(64) Masnovi, J. M.; Kochi, J. K. *J. Am. Chem. Soc.* **1985**, *107*, 7880.

(65) Perrin, D. D.; Armarego, W. L. F.; Perrin, D. R. *Purification of Laboratory Chemicals*, 2nd ed.; Pergamon: Elmsford, NY, 1980.

(66) Kovacic, P.; Sparks, A. K. *J. Am. Chem. Soc.* **1960**, *82*, 5740.

(67) Kochi, J. K.; Bethea, T. W., III *J. Org. Chem.* **1968**, *33*, 75.

(68) Aylett, B. J. In *Comprehensive Inorganic Chemistry*; Bailar, J. C., Jr., Emeleus, J. H., Nyholm, R., Trotman-Dickinson, A. F., Eds.; Pergamon: London, 1973; Vol. 3, p 187.

yields.⁶⁹ No other products were observed. Similarly, durene and mesitylene were cleanly mercurated to single products, 2,3,5,6-tetra-methylphenylmercury(II) trifluoroacetate and 2,4,6-trimethylphenylmercury(II) trifluoroacetate.⁷⁰

The thermal reactions of thallium(III) trifluoroacetate with tri-*tert*-butylbenzene and trineopentylbenzene were carried out in trifluoroacetic acid in the presence of lithium trifluoroacetate as follows. A 1-mL aliquot of 0.03 M $\text{Tl}(\text{O}_2\text{CCF}_3)_3$ was added to a 2-mL aliquot containing tri-*tert*-butylbenzene and lithium trifluoroacetate such that the final concentrations were 0.01 M $\text{Tl}(\text{O}_2\text{CCF}_3)_3$, 0.01 M tri-*tert*-butylbenzene, and 0.05 M lithium trifluoroacetate. The solution was allowed to react overnight at 25 °C in the dark. It was quenched with 2 mL of 1.0 M potassium iodide. Tridecane was added as an internal standard. Iodo-di-*tert*-butylbenzene was obtained in ~10% judging from its mass spectrum: m/z (%) 316 (30), 302 (12), 301 (72), 159 (30), 143 (11), 131 (17), 129 (34), 128 (28), 127 (27), 120 (14), 117 (18), 116 (11), 115 (42), 91 (27), 77 (14), 63 (12), 57 (100). The latter was identical with the product derived from 1,3-di-*tert*-butylbenzene. Two minor products (~5–10%) with GC retention times similar to that of di-*tert*-butylbenzene were observed but not identified. The balance of the tri-*tert*-butylbenzene was recovered intact. No GC/MS corresponding to iodo-di-*tert*-butylbenzene was detected.

In a similar procedure, 1,3,5-trineopentylbenzene⁷¹ afforded ~20% of iodotrineopentylbenzene as judged by GC/MS analysis: m/z (%) 414 (4), 358 (4), 302 (14), 246 (24), 129 (5), 128 (7), 119 (10), 117 (6), 115 (7), 91 (5), 71 (7), 58 (5), 57 (100). The residue was accounted for as unreacted 1,3,5-trineopentylbenzene.

Isolation of Single Crystals for X-ray Crystallographic Analysis. Single crystals of the EDA complex of hexamethylbenzene–mercury(II) trifluoroacetate, 2,4,6-trineopentylphenylmercury(II) trifluoroacetate, and 1,3,5-trineopentylbenzene were obtained by the controlled removal of the solvent. Into a flask with two chambers (connected by a transfer tube with a fine frit) was introduced a concentrated solution of the components. The system was frozen and the contents (in one chamber) were degassed by repeated freeze–pump–thaw cycles. The flask was warmed to room temperature, and only the empty chamber was cooled to 0 °C. The rate of solvent transfer was controlled at ~1.0 mL h⁻¹. The details of the crystal structure of hexamethylbenzene–mercury(II) trifluoro-

acetate have been described earlier.³¹ The details of the crystal structure of 2,4,6-trineopentylphenylmercury(II) trifluoroacetate and 1,3,5-trineopentylbenzene illustrated in Figures 10 and 15 are included in the supplementary material.

Acknowledgment. We thank S. Fukuzumi for helpful suggestions, J. C. Huffman for the crystal structures in Figures 10 and 15, and the National Science Foundation and Robert A. Welch Foundation for financial support.

Registry No. $[(\text{CH}_3)_6\text{C}_6\text{H}_6\text{Hg}(\text{O}_2\text{CCF}_3)_2]$, 77001-38-8; $[(\text{CH}_3)_3\text{C}_6\text{H}_4\text{Hg}(\text{O}_2\text{CCF}_3)_2]$, 103621-77-8; $[1,2,4,5-(\text{CH}_3)_4\text{C}_6\text{H}_2\text{Hg}(\text{O}_2\text{CCF}_3)_2]$, 78717-21-2; $[1,2,3,5-(\text{CH}_3)_4\text{C}_6\text{H}_2\text{Hg}(\text{O}_2\text{CCF}_3)_2]$, 103621-78-9; $[1,2,3,4-(\text{CH}_3)_4\text{C}_6\text{H}_2\text{Hg}(\text{O}_2\text{CCF}_3)_2]$, 78717-15-4; $[1,2,3-(\text{CH}_3)_3\text{C}_6\text{H}_3\text{Hg}(\text{O}_2\text{CCF}_3)_2]$, 103621-79-0; $[1,2,4-(\text{CH}_3)_3\text{C}_6\text{H}_3\text{Hg}(\text{O}_2\text{CCF}_3)_2]$, 103621-80-3; $[1,3,5-(\text{CH}_3)_3\text{C}_6\text{H}_3\text{Hg}(\text{O}_2\text{CCF}_3)_2]$, 78717-11-0; $[1,2-(\text{C}_6\text{H}_5)_2\text{C}_6\text{H}_4\text{Hg}(\text{O}_2\text{CCF}_3)_2]$, 78716-61-7; $[\text{H}_3\text{CC}_6\text{H}_5\text{Hg}(\text{O}_2\text{CCF}_3)_2]$, 78716-26-4; $[\text{C}_6\text{H}_5\text{Hg}(\text{O}_2\text{CCF}_3)_2]$, 78716-15-1; $[(\text{CH}_3)_6\text{C}_6\text{Ti}(\text{O}_2\text{CCF}_3)_3]$, 92397-33-6; $[(\text{C}_6\text{H}_5)_6\text{C}_6\text{Ti}(\text{O}_2\text{CCF}_3)_3]$, 92397-34-7; $[(\text{CH}_3)_5\text{C}_6\text{HTi}(\text{O}_2\text{CCF}_3)_3]$, 92397-35-8; $[1,2,3,4-(\text{CH}_3)_4\text{C}_6\text{H}_2\text{Ti}(\text{O}_2\text{CCF}_3)_3]$, 92397-36-9; $[1,2,3,5-(\text{CH}_3)_4\text{C}_6\text{H}_2\text{Ti}(\text{O}_2\text{CCF}_3)_3]$, 92397-37-0; $[1,2,4,5-(\text{CH}_3)_4\text{C}_6\text{H}_2\text{Ti}(\text{O}_2\text{CCF}_3)_3]$, 92397-38-1; $[1,2,3-(\text{CH}_3)_3\text{C}_6\text{H}_3\text{Ti}(\text{O}_2\text{CCF}_3)_3]$, 92397-39-2; $[1,2,4-(\text{CH}_3)_3\text{C}_6\text{H}_3\text{Ti}(\text{O}_2\text{CCF}_3)_3]$, 92397-40-5; $[1,3,5-(\text{CH}_3)_3\text{C}_6\text{H}_3\text{Ti}(\text{O}_2\text{CCF}_3)_3]$, 92397-41-6; $[1,2-(\text{CH}_3)_2\text{C}_6\text{H}_4\text{Ti}(\text{O}_2\text{CCF}_3)_3]$, 92397-42-7; $[1,3-(\text{CH}_3)_2\text{C}_6\text{H}_4\text{Ti}(\text{O}_2\text{CCF}_3)_3]$, 92397-43-8; $[1,4-(\text{CH}_3)_2\text{C}_6\text{H}_4\text{Ti}(\text{O}_2\text{CCF}_3)_3]$, 92420-19-4; $[t\text{-C}_4\text{H}_9\text{C}_6\text{H}_5\text{Ti}(\text{O}_2\text{CCF}_3)_3]$, 92397-44-9; $[i\text{-C}_4\text{H}_9\text{C}_6\text{H}_5\text{Ti}(\text{O}_2\text{CCF}_3)_3]$, 92397-45-0; $[\text{C}_2\text{H}_5\text{C}_6\text{H}_5\text{Ti}(\text{O}_2\text{CCF}_3)_3]$, 92397-46-1; $[\text{H}_3\text{CC}_6\text{H}_5\text{Ti}(\text{O}_2\text{CCF}_3)_3]$, 92397-47-2; $[\text{C}_6\text{H}_5\text{Ti}(\text{O}_2\text{CCF}_3)_3]$, 92397-48-3; $1,3,5-(\text{CH}_3)_3\text{C}_6\text{H}_3$, 108-67-8; $1,2,4-(\text{CH}_3)_3\text{C}_6\text{H}_3$, 95-63-6; $1,2,3-(\text{CH}_3)_3\text{C}_6\text{H}_3$, 526-73-8; $1,2,3,4-(\text{CH}_3)_4\text{C}_6\text{H}_2$, 488-23-3; $1,2,3,5-(\text{CH}_3)_4\text{C}_6\text{H}_2$, 527-53-7; $1,2,4,5-(\text{CH}_3)_4\text{C}_6\text{H}_2$, 95-93-2; $(\text{CH}_3)_3\text{C}_6\text{H}$, 700-12-9; $1,3-(\text{CH}_3)_2\text{C}_6\text{H}_4$, 108-38-3; $1,4-(\text{CH}_3)_2\text{C}_6\text{H}_4$, 106-42-3; $1,2-(\text{CH}_3)_2\text{C}_6\text{H}_4$, 95-47-6; $t\text{-C}_4\text{H}_9\text{C}_6\text{H}_5$, 98-06-6; $i\text{-C}_4\text{H}_9\text{C}_6\text{H}_5$, 98-82-8; $\text{C}_2\text{H}_5\text{C}_6\text{H}_5$, 100-41-4; $\text{CH}_3\text{C}_6\text{H}_5$, 108-88-3; C_6H_6 , 71-43-2; ClC_6H_5 , 108-90-7; D, 16873-17-9; $\text{F}_3\text{CCO}_2\text{H}\cdot\text{H}^{1/2}\text{Hg}^{\text{II}}$, 13257-51-7; $\text{F}_3\text{CCO}_2\text{H}\cdot\text{H}^{1/3}\text{Tl}^{\text{III}}$, 23586-53-0; $((\text{CH}_3)_3\text{CCH}_2)_3\text{C}_6\text{H}_3$, 21411-39-2; $((\text{CH}_3)_3\text{CC}_6\text{H}_2)_3\text{C}_6\text{H}_2\text{HgO}_2\text{CCF}_3$, 103621-81-4.

Supplementary Material Available: Data collection, processing parameters and positional parameters for X-ray crystallography of 2,4,6-trineopentylphenylmercury(II) trifluoroacetate and 1,3,5-trineopentylbenzene (6 pages). Ordering information is given on any current masthead page.

Asymmetric Oxidoreductions Catalyzed by Alcohol Dehydrogenase in Organic Solvents¹

Jacob Grunwald,[†] Beat Wirz,[‡] Mark P. Scollar, and Alexander M. Klibanov*

Contribution from the Department of Applied Biological Sciences, Massachusetts Institute of Technology, Cambridge, Massachusetts 02139. Received April 4, 1986

Abstract: A methodology is developed for the use of alcohol dehydrogenase (and other NAD⁺/NADH-dependent enzymes) as catalysts in organic solvents. The enzyme and the cofactor are deposited onto the surface of glass beads which are then suspended in a water-immiscible organic solvent containing the substrate. Both NADH and NAD⁺ are efficiently regenerated in such a system with alcohol dehydrogenase-catalyzed oxidation of ethanol and reduction of isobutyraldehyde, respectively; cofactor turnover numbers of 10⁵ to greater than 10⁶ have been obtained. With use of asymmetric oxidoreductions catalyzed by horse liver alcohol dehydrogenase in isopropyl ether, optically active (ee of 95 to 100%) alcohols and ketones have been prepared on a 1 to 10 mmol scale.

The use of alcohol dehydrogenases (ADH) for preparative production of optically active alcohols and ketones has received much attention² due to the importance of asymmetric carbonyl/alcohol oxidoreductions in organic chemistry³. Despite some impressive successes,⁴ this synthetic strategy still has serious practical drawbacks such as operational instability of most ADH^{2b} and their cofactor NADH,⁵ insolubility of most of their substrates in water which necessitates work in emulsions or suspensions, product inhibition of the enzyme,^{4c} and lability of some substrates and products of ADH in aqueous solutions.⁶

We have recently employed enzymes for preparative transformations in organic solvents instead of water.⁷ Although this

(1) This paper is dedicated to the memory of Professor Nathan O. Kaplan who passed away on April 15 of this year. Dr. Kaplan, a pioneer in many areas of biochemistry, made a number of pivotal and insightful contributions to dehydrogenase enzymology.

(2) (a) Prelog, V. *Pure Appl. Chem.* **1964**, *9*, 119–130. (b) Jones, J. B.; Beck, J. F. In *Applications of Biochemical Systems in Organic Chemistry*; Jones, J. B., Sih, C. J., Perlman, D., Eds., Wiley: New York, 1976; Part 1, pp 107–401. (c) May, S. W.; Padgett, S. R. *Bio/Technology* **1983**, *1*, 677–686. (d) Whitesides, G. M.; Wong, C.-H. *Angew. Chem., Int. Ed. Engl.* **1985**, *24*, 617–638. (e) Jones, J. B. *Tetrahedron* **1986**, *42*, 3351–3403.

[†] On leave from Israel Institute for Biological Research, Ness-Ziona, Israel.

[‡] On leave from F. Hoffmann-La Roche & Co., Basel, Switzerland.